Electronic Supplementary Material (ESI) for Chemical Science

Supporting Information

Stimuli-Responsive Pd_2L_4 Metallosupramolecular Cages: Towards Targeted Cisplatin Drug Delivery.

James E. M. Lewis,[a] Emma L. Gavey,[a] Scott A. Cameron,[a] and James D. Crowley[a]*

[a]Department of Chemistry, University of Otago, PO Box 56, Dunedin,

New Zealand; Fax: +64 3 479 7906; Tel: +64 3 479 7731.

***jcrowley@chemistry.otago.ac.nz**

Contents

1 Experimental Procedures

1.1 General

Unless otherwise stated, all reagents were purchased from commercial sources and used without further purification. ^{1}H and ^{13}C NMR spectra were recorded on either a 400 MHz Varian 400 MR or Varian 500 MHz VNMRS spectrometer. Chemical shifts are reported in parts per million and referenced to residual solvent peaks ($CDCl_3$: ^{1}H δ 7.26 ppm, ^{13}C δ 77.16 ppm; CD_3CN: ^{1}H δ 1.94, ^{13}C δ 1.32, 118.26 ppm, d_6-DMSO: ^{1}H δ 2.50 ppm; ^{13}C δ 39.52 ppm). Coupling constants (J) are reported in Hertz (Hz). Standard abbreviations indicating multiplicity were used as follows: m = multiplet, q = quartet, t = triplet, dt = double triplet, d = doublet, dd = double doublet, s = singlet. IR spectra were recorded on a Bruker ALPHA FT-IR spectrometer with an attached ALPHA-P measurement module. Microanalyses were performed at the Campbell Microanalytical Laboratory at the University of Otago. Electrospray mass spectra (ESMS) were collected on a Bruker micro-TOF-Q spectrometer. UV-visible absorption spectra were acquired with a Perkin Elmer Lambda-950 spectrophotometer.

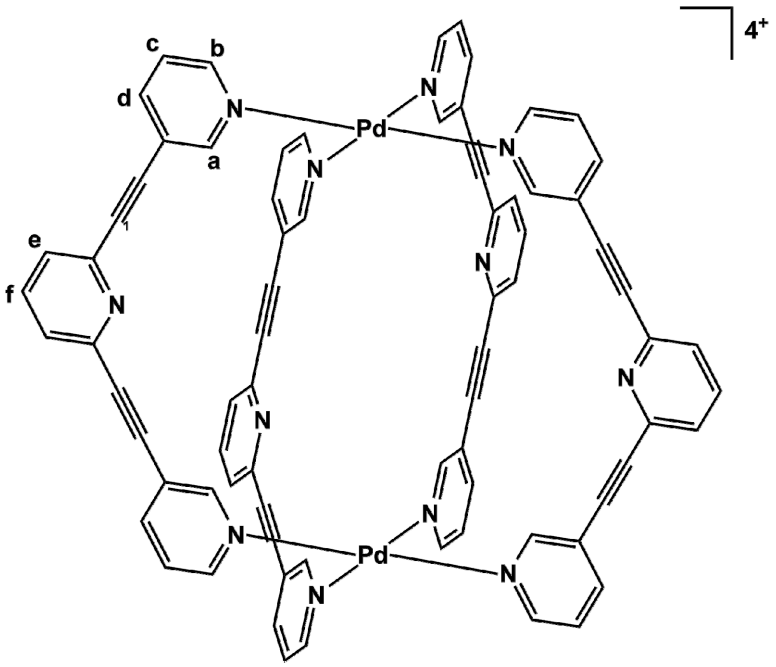

Figure S1: Labelling scheme for **2**$(X)_4$.

1.2 Synthesis of 2$(BF_4)_4$

To a stirring solution of **1** (0.141 g, 0.50 mmol, 2 eq.) in acetonitrile (10 mL) was added dropwise a solution of $[Pd(CH_3CN)_4](BF_4)_2$ (0.111 g, 0.25 mmol, 1 eq.) in acetonitrile (5 mL). The resulting solution was stirred at room temperature for 1 hour before filtering through cotton wool and the product precipitated by vapour diffusion of diethyl ether over 36 hours. The supernatant was decanted off and the solid dried *in vacuo* to give **2**$(BF_4)_4$ as a tan solid. Yield 0.200 g (0.12 mmol, 95%). ^{1}H NMR (400 MHz, d_6-DMSO) δ: 9.54 (s, 2H, H_a), 9.38 (dd, J = 1.5, 5.9 Hz, 2H, H_b), 8.35 (dt, J = 1.5, 8.2 Hz, 2H, H_d), 8.01 (t, J = 7.5 Hz, 1H, H_f), 7.86 (dd, J = 5.9, 8.1 Hz, 2H, H_c), 7.79 (d, J = 7.8 Hz, 2H, H_e). ^{1}H NMR (400 MHz, CD_3CN) δ: 9.34 (d, J = 1.5 Hz, 2H, H_a), 9.08 (dd, J = 1.2, 5.8 Hz, 2H, H_b), 8.17 (dt, J = 1.4, 8.0 Hz, 2H, H_d), 7.87 (t, J = 7.8 Hz, 1H, H_f), 7.68 (d, J = 7.8 Hz, 2H, H_e), 7.66 (dd, J = 5.8, 8.0

Hz, 2H, H_c). ^{13}C NMR (500 MHz, d_6-DMSO) δ: 153.3 (C_a), 151.1(C_b), 143.5 (C_d), 141.8, 138.3 (C_f), 128.6 (C_e), 127.4 (C_c), 121.5, 93.3, 83.6. IR (ATR): υ (cm^{-1}) 3087, 1575, 1558, 1483, 1444, 1420, 1199, 1046, 803, 727, 690, 572, 558, 520. HRESI-MS (CH_3CN): *m/z* = 1598.1482 $[Pd_2(C_{19}H_{11}N_3)_4(BF_4)_3]^+$ calc. 1598.2022; 756.0795 $[Pd_2(C_{19}H_{11}N_3)_4(BF_4)_2]^{2+}$ calc. 756.0989. UV-Vis (DMSO, ε [$M^{-1}cm^{-1}$]): λ_{max} nm = 314 (1.02×10^5), 268 (1.20×10^5). *Anal.* Calc for **2**$(BF_4)_4.(CH_3CN)_3(H_2O)_3$: C, 52.88; H, 3.19; N, 11.28%. Found: C, 52.67; H, 3.02; N, 11.40%.

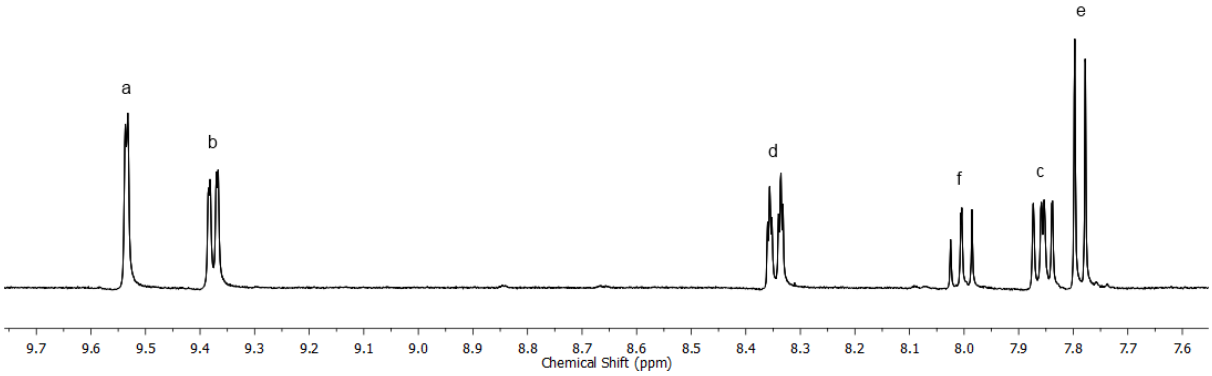

Figure S2: ^1H NMR (400 MHz, d_6-DMSO) spectrum for **2**$(BF_4)_4$.

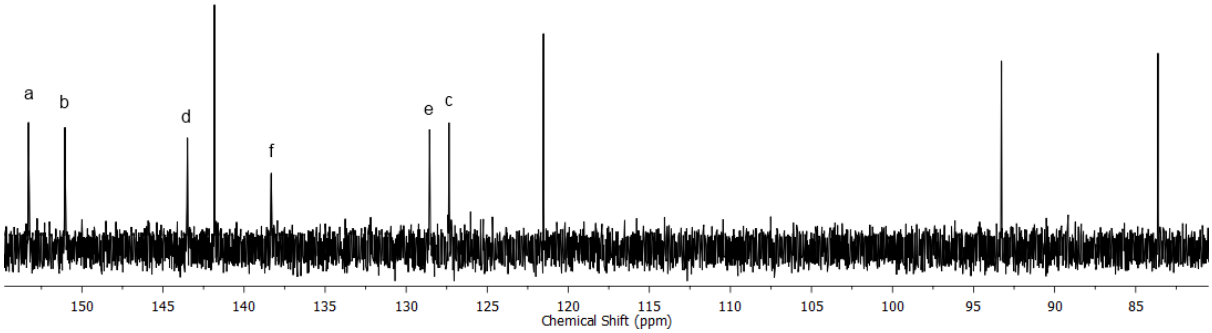

Figure S3: ^{13}C NMR (500 MHz, d_6-DMSO) spectrum for **2**$(BF_4)_4$.

1.3 Synthesis of 2$(SbF_6)_4$

$AgSbF_6$ (0.172 g, 0.50 mmol, 2 eq.) and $Pd(CH_3CN)_2Cl_2$ (0.065 g, 0.25 mmol, 1 eq.) were stirred in acetone (dry, 10 mL) under N_2 in the dark for 30 minutes. The reaction was filtered through celite (dried in oven) to give a red solution that was added dropwise to a stirring solution of **1** (0.141 g, 0.50 mmol, 2 eq.) in acetone (dry, 10 mL). After stirring for 1 hour the reaction solution was filtered through cotton wool and the product precipitated by vapour diffusion of diethyl ether over 48 hours. The supernatant was decanted off and the solid dried *in vacuo* to give **2**$(SbF_6)_4$ as a tan solid. Yield 0.225 g (0.10 mmol, 79%). ^1H NMR (400 MHz, CD_3CN) δ: 9.27 (s, 2H, H_a), 9.00 (dd, J = 1.1, 5.9 Hz, 2H, H_b), 8.17 (dt, J = 1.5, 8.1 Hz, 2H, H_d), 7.87 (t, J = 8.2 Hz, 1H, H_f), 7.68 (d, J = 7.8 Hz, 2H, H_e), 7.66 (dd, J = 5.8, 7.6 Hz, 2H, H_c). ^{13}C NMR (400 MHz, CD_3CN) δ: 154.5 (C_a), 151.4 (C_b), 144.5 (C_d), 143.3, 138.7 (C_f), 129.4 (C_e), 128.5 (C_c), 124.1, 94.6, 83.5. IR (ATR): υ (cm^{-1}) 3069, 1579, 1557, 1482, 1448, 1417, 1239, 811, 696. HRESI-MS (CH_3CN/CH_3OH): *m/z* = 2044.8478 $[Pd_2(C_{19}H_{11}N_3)_4(SbF_6)_3]^+$ calc. 2044.8741; 904.9749 $[Pd_2(C_{19}H_{11}N_3)_4(SbF_6)_2]^{2+}$ calc. 904.9897. UV-Vis (DMSO, ε [$M^{-1}cm^{-1}$]): λ_{max} nm = 317 (9.10×10^4), 270 (1.05×10^5). *Anal.* Calc for **2**$(SbF_6)_4.(CH_3COCH_3)_5$: C, 42.50; H, 2.90; N, 6.54%. Found: C, 42.70; H, 3.11; N, 6.40%.

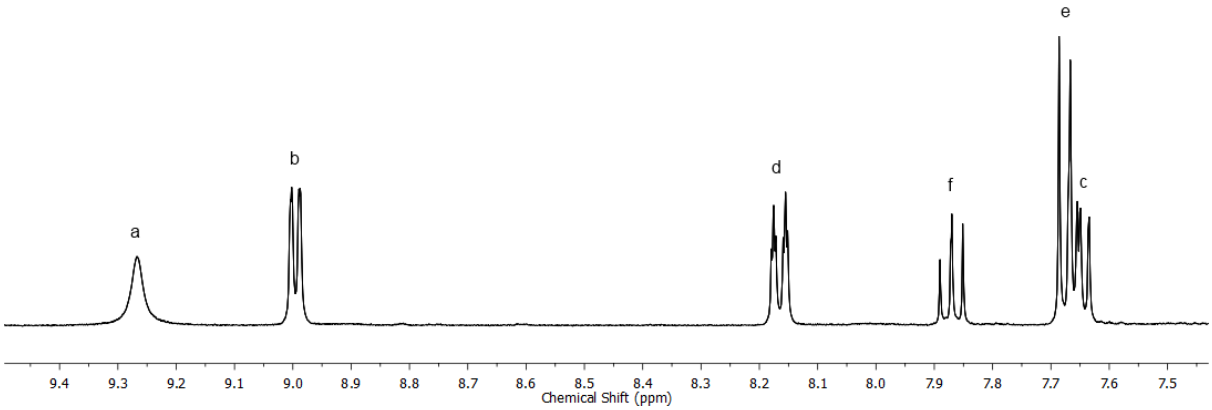

Figure S4: ^{1}H NMR (400 MHz, CD_3CN) spectrum for **2**$(SbF_6)_4$.

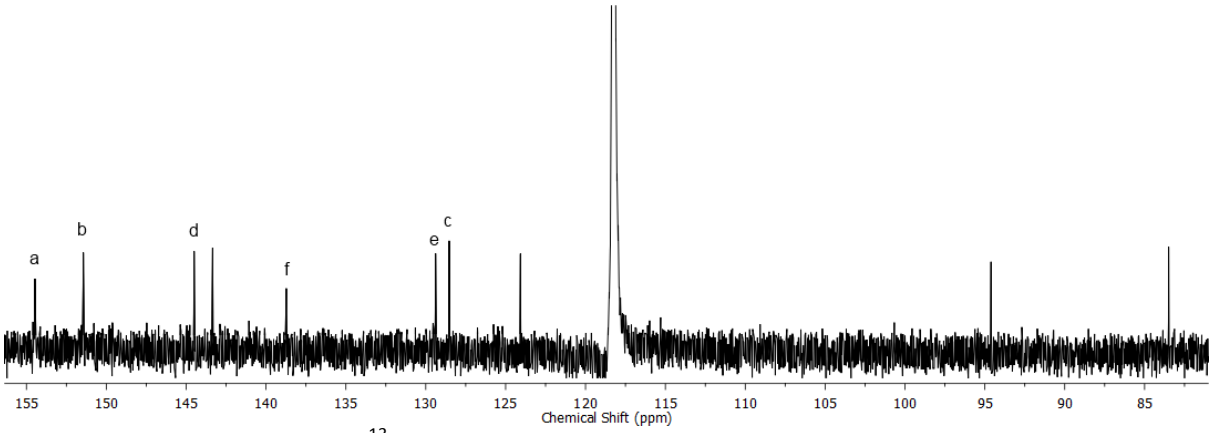

Figure S5: ^{13}C NMR (400 MHz, CD_3CN) spectrum for **2**$(SbF_6)_4$.

1.4 Synthesis of $[Pd(DMAP)_4](BF_4)_2$

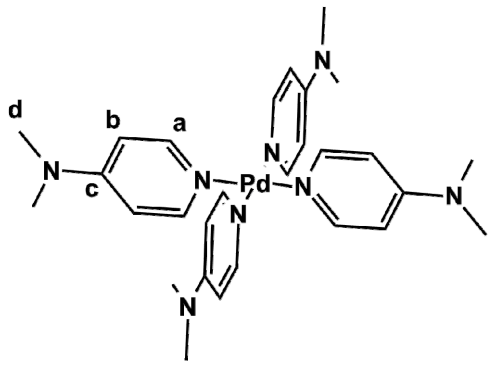

Figure S6: Labelling scheme for $[Pd(DMAP)_4](BF_4)_2$.

$[Pd(CH_3CN)_4](BF_4)_2$ (0.022 g, 0.05 mmol, 1 eq.) and 4-dimethylaminopyridine (0.024 g, 0.2 mmol, 4 eq.) were stirred in acetonitrile (2.5 mL) for 30 minutes. The product was precipitated as a light yellow crystalline solid by vapour diffusion of diethyl ether over a period of 24 hours. Yield 0.032 g (0.04 mmol, 84%). ^{1}H NMR (400 MHz, d_6-DMSO) δ: 8.22 (d, J = 7.1 Hz, 2H, H_a), 6.71 (d, J = 7.3 Hz, 2H, H_b), 2.96 (s, 6H, H_d). ^{1}H NMR (400 MHz, CD_3CN) δ: 7.97 (d, J = 7.4 Hz, 2H, H_a), 6.55 (d, J = 7.4 Hz, 2H, H_b), 2.98 (s, 6H, H_d). ^{13}C NMR (400 MHz, CD_3CN) δ: 156.1 (C_a), 150.0 (C_b), 109.2 (C_c), 39.59 (C_d). IR (ATR): υ (cm^{-1}) 1617, 1544, 1444, 1392, 1351, 1224, 1049, 1017, 944, 806, 520. HRESI-MS (MeCN):

m/z = 681.2381 $[Pd(C_7H_{10}N_2)_4(BF_4)]^+$ calc. 681.2449; 297.1205 $[Pd(C_7H_{10}N_2)4]^{2+}$ calc. 297.1196. *Anal*. Calc for $C_{28}H_{40}B_2F_8Pd$: C, 43.75; H, 5.24; N, 14.58%. Found: C, 44.05; H, 5.36; N, 14.67%.

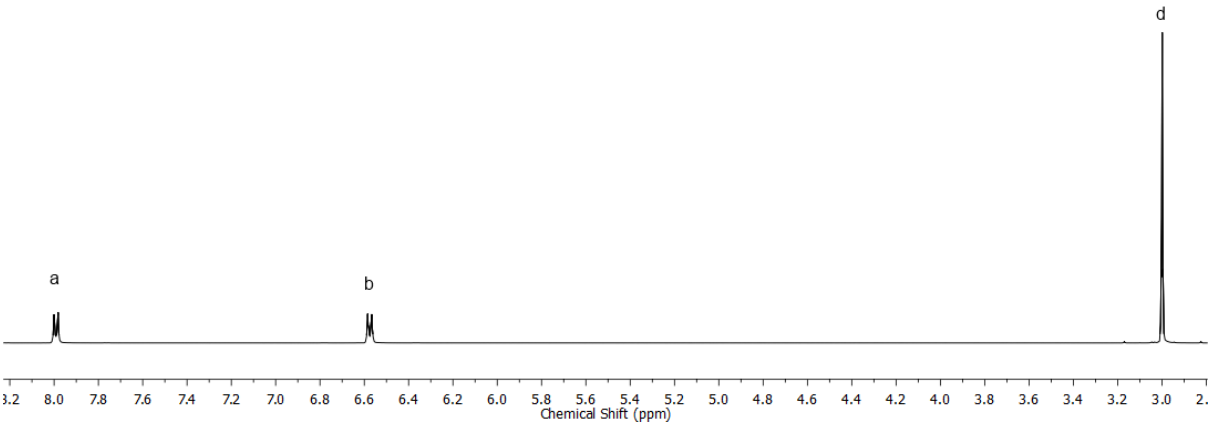

Figure S7: ^{1}H NMR (400 MHz, CD_3CN) spectrum for $[Pd(DMAP)_4](BF_4)_2$.

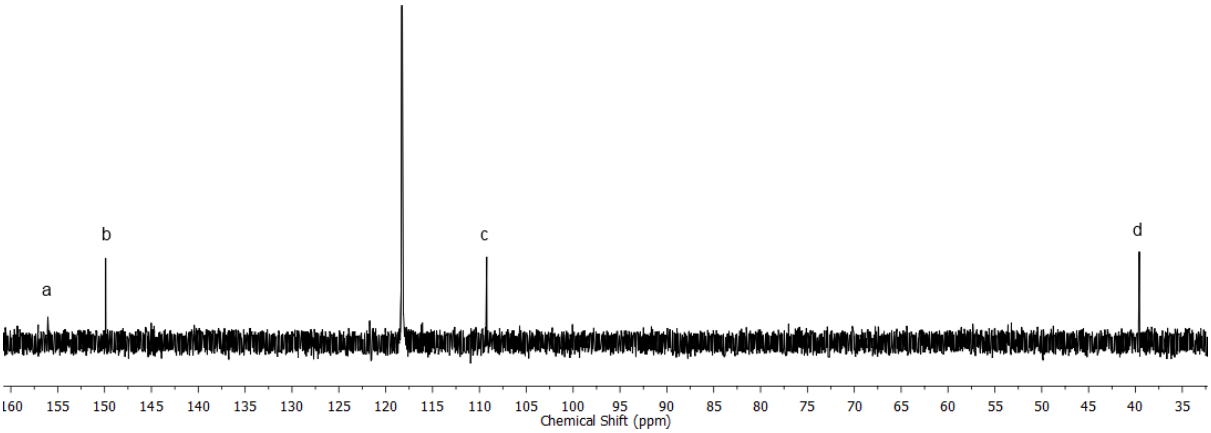

Figure S8: ^{13}C NMR (400 MHz, CD_3CN) spectrum for $[Pd(DMAP)_4](BF_4)_2$.

1.5 Synthesis of $[Pd_2(S1)_4](BF_4)_4$

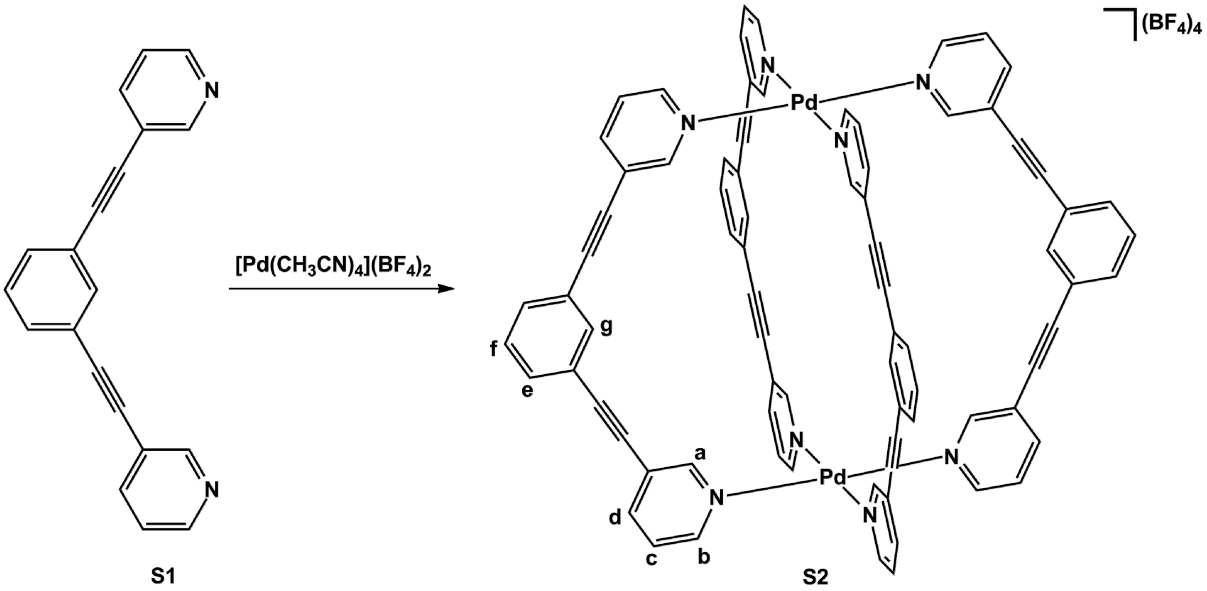

Figure S9: Self-assembly of cage complex **S2** from ligand **S1**.

To a stirring solution of $[Pd(CH_3CN)_4](BF_4)_2$ (0.66 g, 1.49 mmol, 1 eq.) in acetonitrile (dry, 5 mL) was added **S1** (0.833 g, 2.97 mmol, 2 eq.). The reaction mixture was heated at 50 °C for 30 minutes. The product was precipitated as a pale yellow solid by vapour diffusion of diethyl ether into the cooled reaction mixture. Yield 0.98 g (0.58 mmol, 78%). ^{1}H NMR (400 MHz, d_6-DMSO) δ: 9.60 (s, 2H, H_a), 9.36 (d, J = 5.0 Hz, 2H, H_b), 8.28 (d, J = 8.0 Hz, 2H, H_d), 7.95 (s, 2H, H_g), 7.82 (dd, J = 5.9, 7.9 Hz, 2H, H_c), 7.73 (dd, J = 1.4, 7.9 Hz, 2H, H_e), 7.58 (t, J = 7.8, 1H, H_f). ^{13}C NMR (400 MHz, d_6-DMSO) δ: 153.2, 151.1, 143.5, 141.8, 138.3, 128.6, 127.4, 121.6, 109.6, 93.3, 83.6. IR (ATR): υ (cm^{-1}) 3566, 3210, 1718, 1600, 1562, 1488, 1413, 1295, 1198, 1163, 1050, 809, 796, 680, 520, 418. HRESI-MS (CH_3CN/CH_3OH): *m/z* = 1594.2218 $[Pd_2(C_{20}H_{12}N_2)_4(BF_4)_3]^+$ calc. 1594.2213; 754.1044 $[Pd_2(C_{20}H_{12}N_2)_4(BF_4)_2]^{2+}$ calc. 754.1085; 333.5552 $[Pd_2(C_{20}H_{12}N_2)_4]^{4+}$ calc. 333.5521. UV-Vis (DMSO, ε [$M^{-1}\cdot cm^{-1}$]): λ_{max} nm = 286 (1.75×10^5). *Anal*. Calc for $C_{80}H_{48}N_8B_4F_{16}Pd$: C, 61.01; H, 3.03; N, 7.11%. Found: C, 53.45; H, 3.03; N, 6.18%.

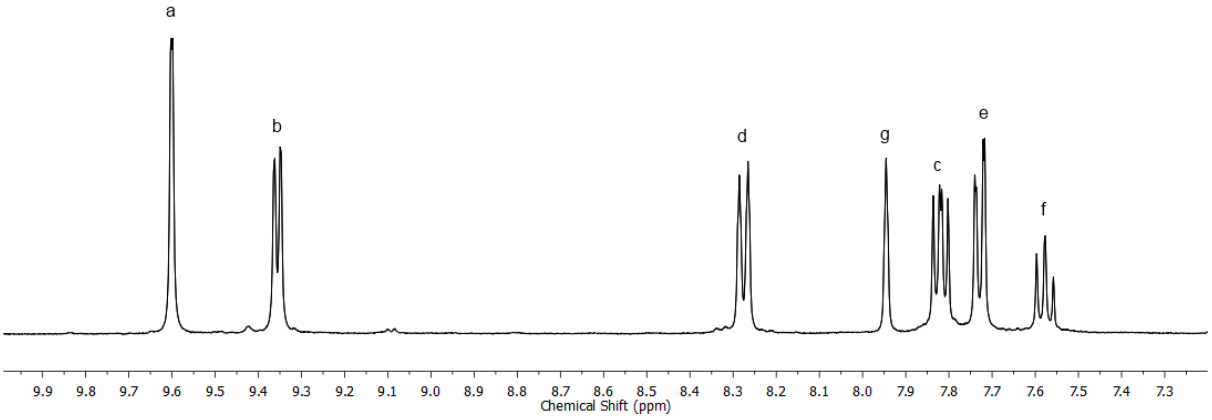

Figure S10: ^{1}H NMR (400 MHz, d_6-DMSO) spectrum for **S2**.

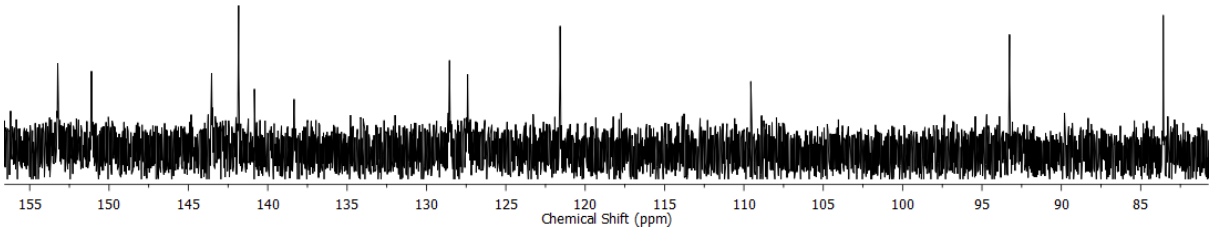

Figure S11: ^{13}C NMR (400 MHz, d_6-DMSO) spectrum for **S2**.

2 ^{1}H DOSY NMR Spectra

2.1 ^{1}H DOSY NMR spectrum of 1 (CD_3CN, 298 K)

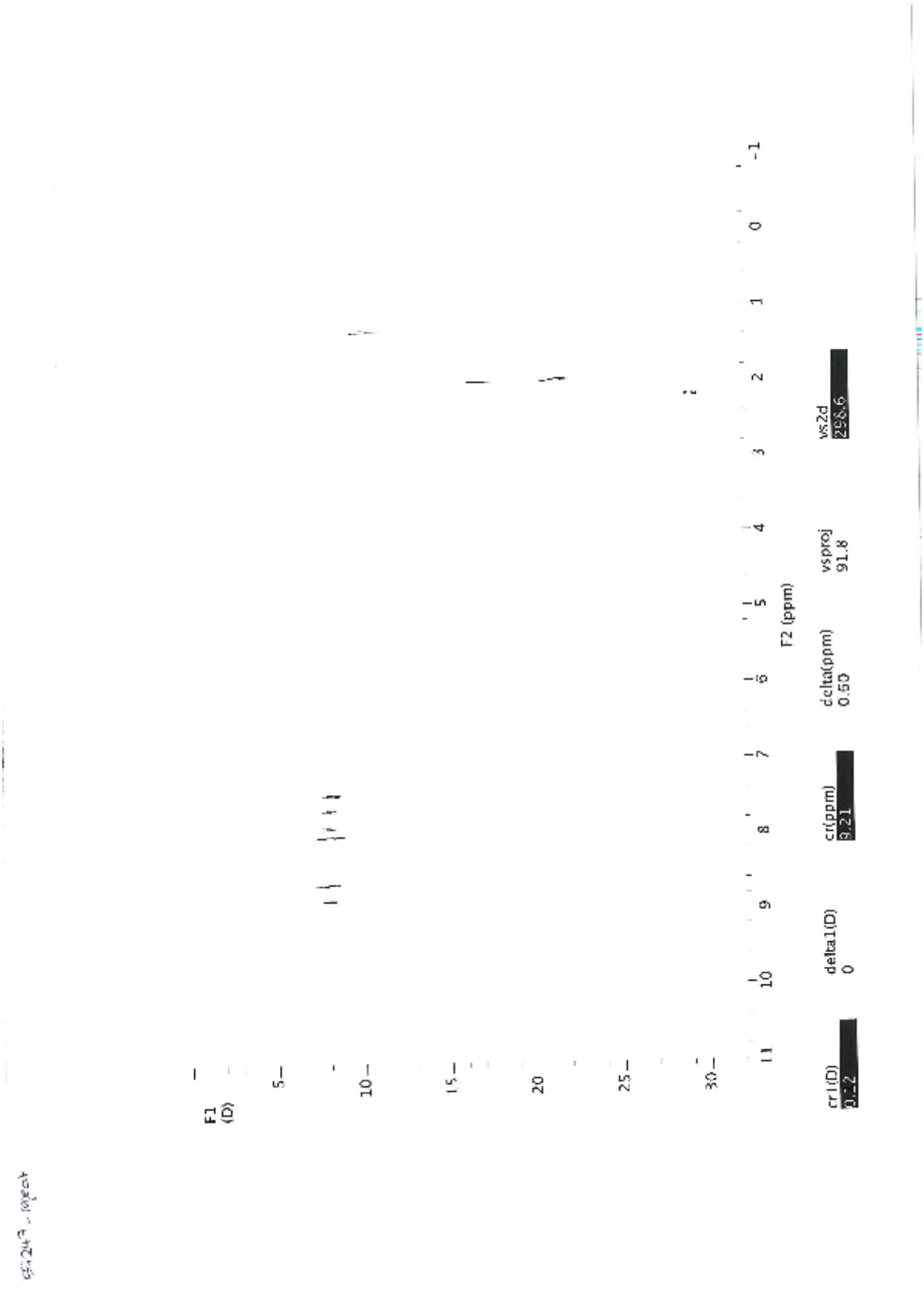

2.2 ^{1}H DOSY NMR spectrum of 2$(BF_4)_4$ (CD_3CN, 298 K)

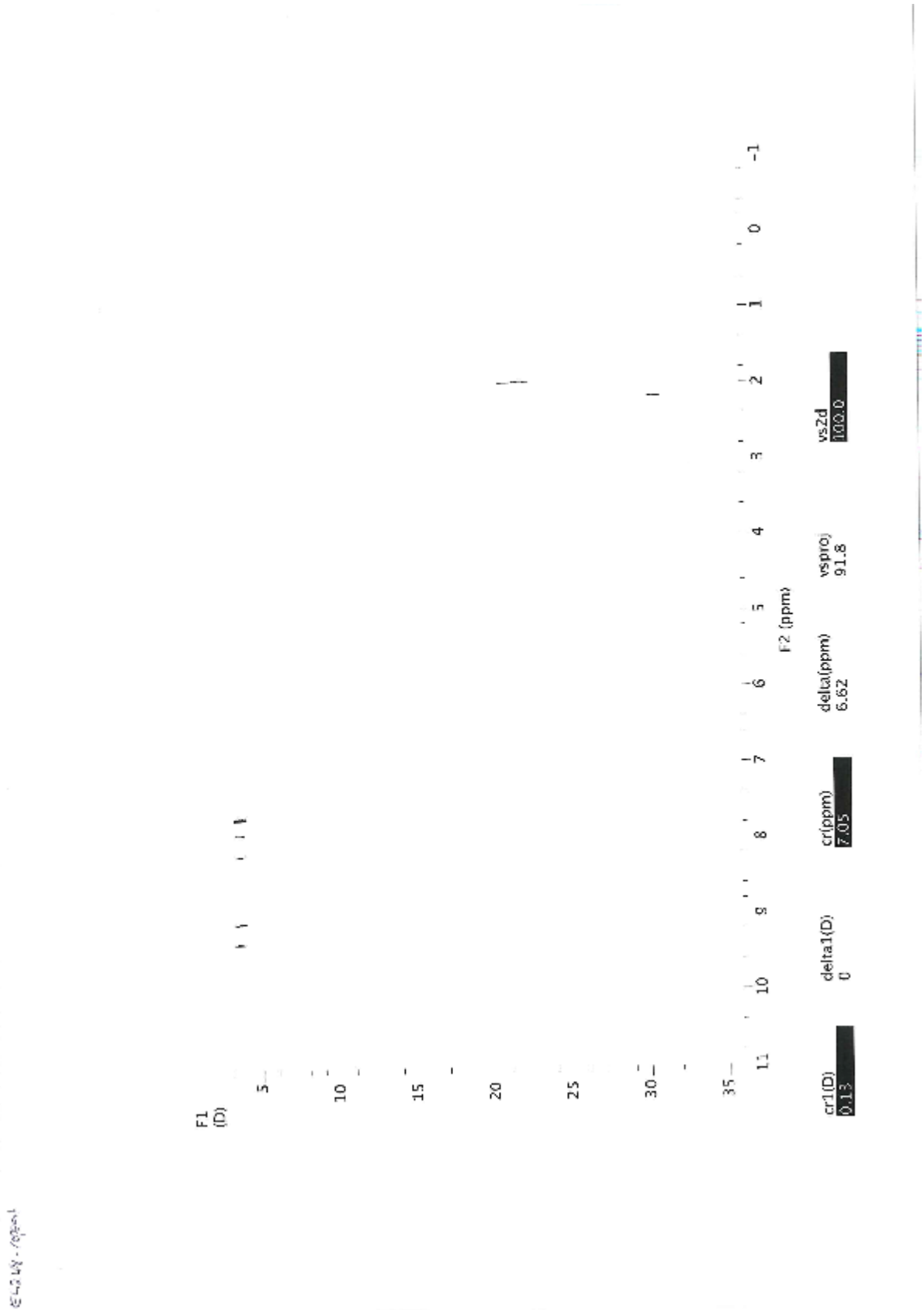

2.3 ^{1}H DOSY NMR spectrum of 2$(SbF_6)_4$ (CD_3CN, 298 K)

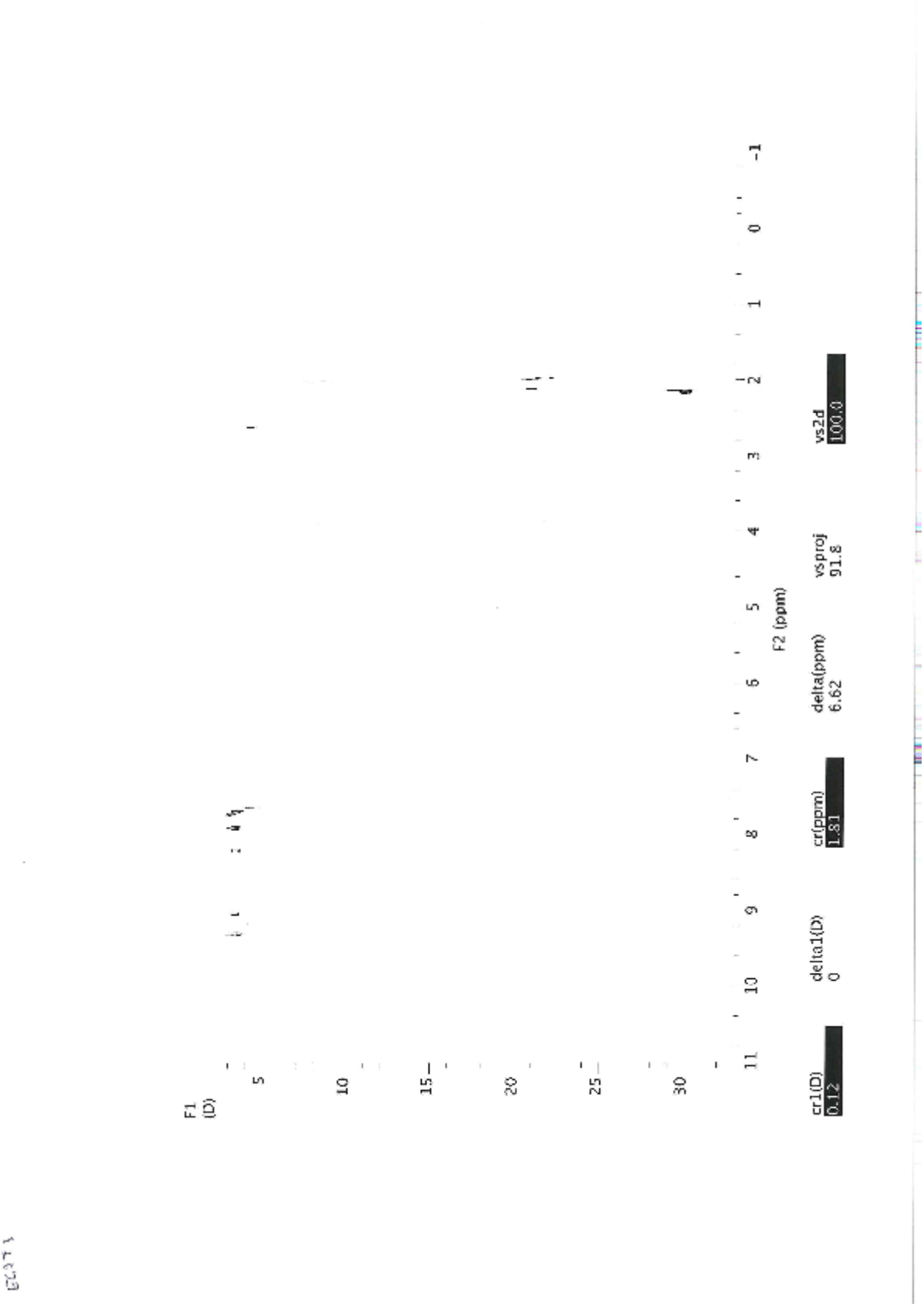

3 Mass Spectra

3.1 Mass Spectra of $2(BF_4)_4$

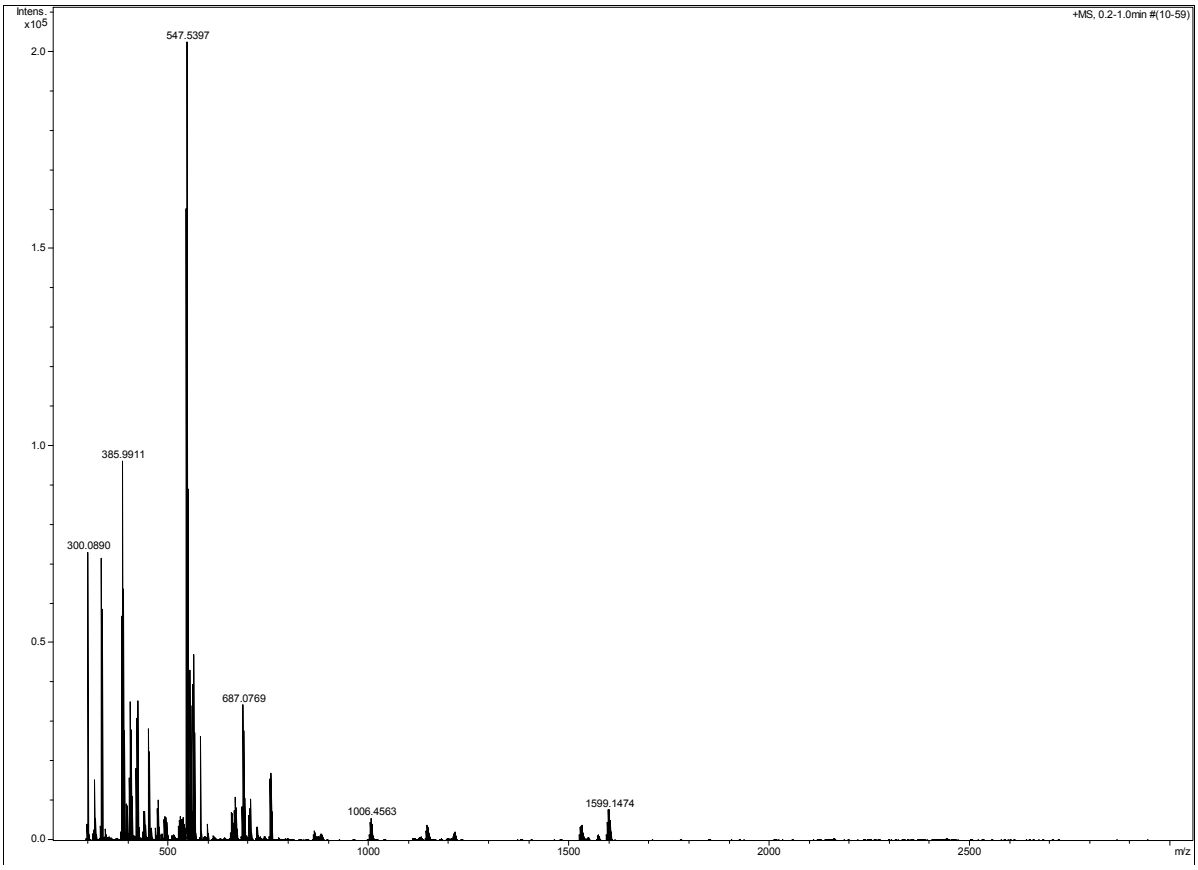

Figure S12: HR-ESI Mass Spectrum (+ve ion, MeCN) of **2**$(BF_4)_4$. *m/z* = 1598.1482 $[Pd_2(\mathbf{1})_4(BF_4)_3]^+$; 756.0795 $[Pd_2(\mathbf{1})_4(BF_4)_2]^{2+}$.

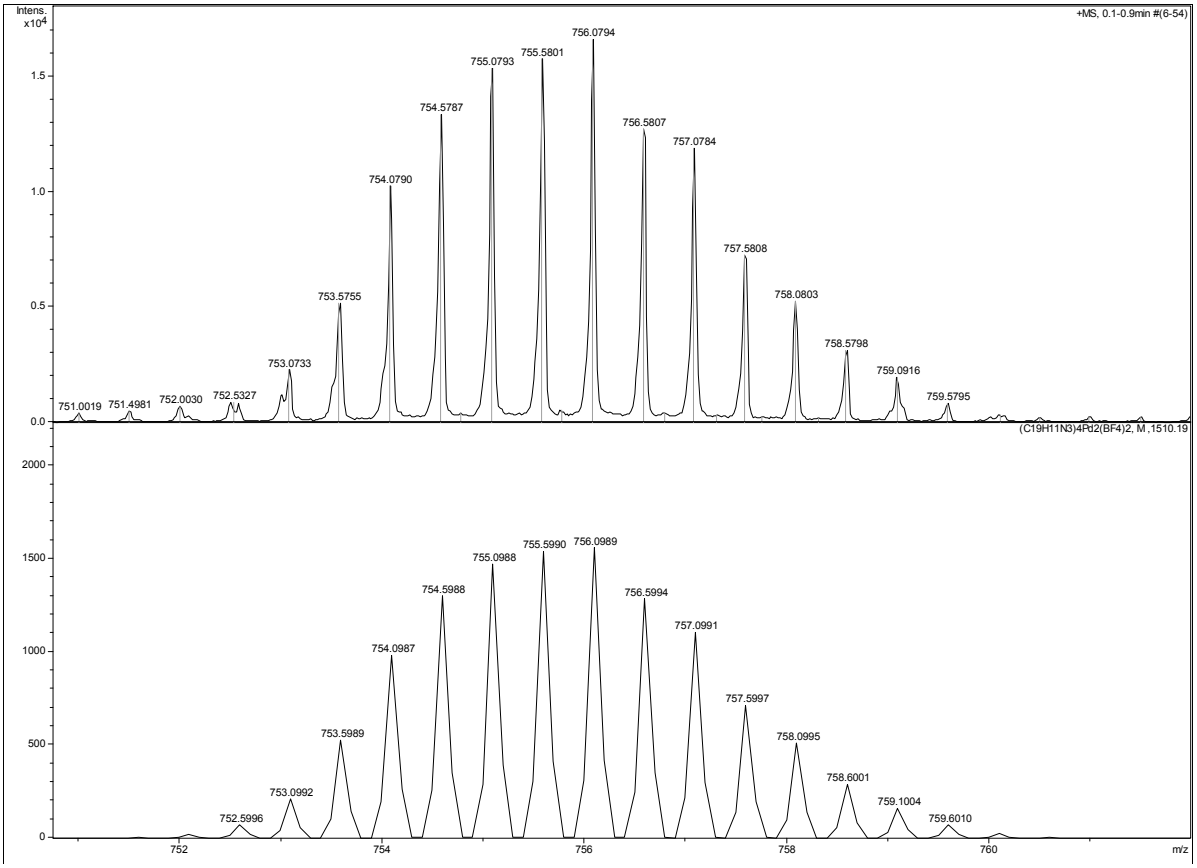

Figure S13: Experimental (top) and theoretical (bottom) isotope patterns for $[Pd_2(\mathbf{1})_4(BF_4)_3]^+$.

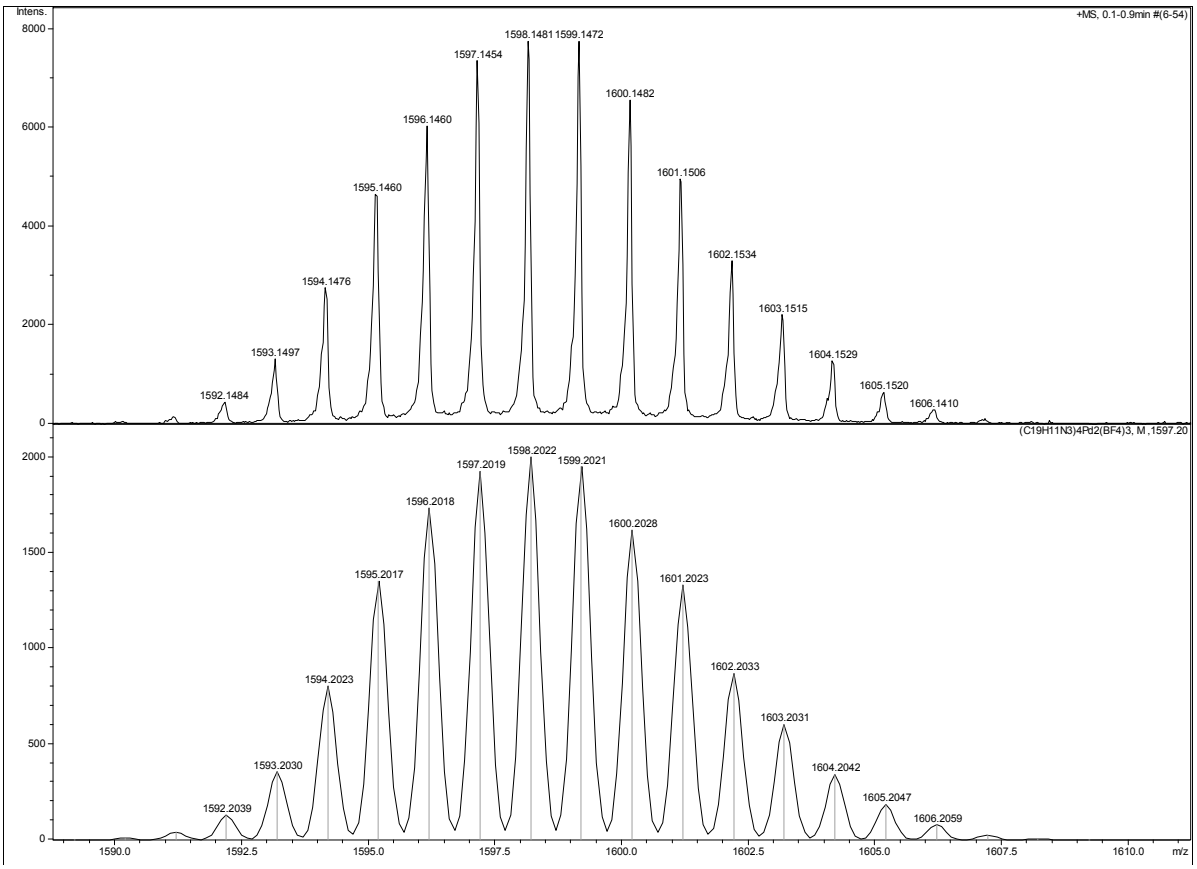

Figure S14: Experimental (top) and theoretical (bottom) isotope patterns for $[Pd_2(\mathbf{1})_4(BF_4)_2]^{2+}$.

3.2 Mass Spectra of $2(SbF_6)_4$

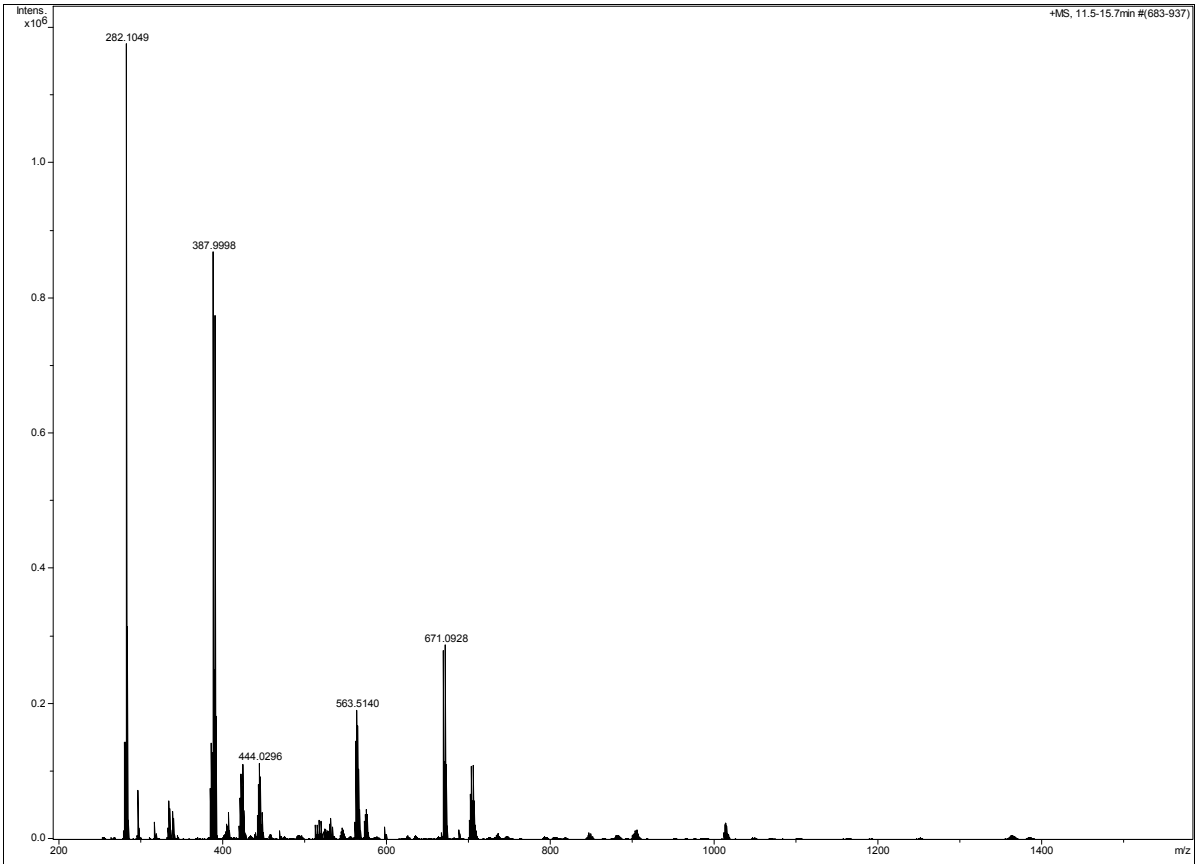

Figure S15: HR-ESI Mass Spectrum (+ve ion, MeCN) of **2**$(SbF_6)_4$. *m/z* = 2044.8478 $[Pd_2(\mathbf{1})_4(SbF_6)_3]^+$; 904.9749 $[Pd_2(\mathbf{1})_4(SbF_6)_2]^{2+}$.

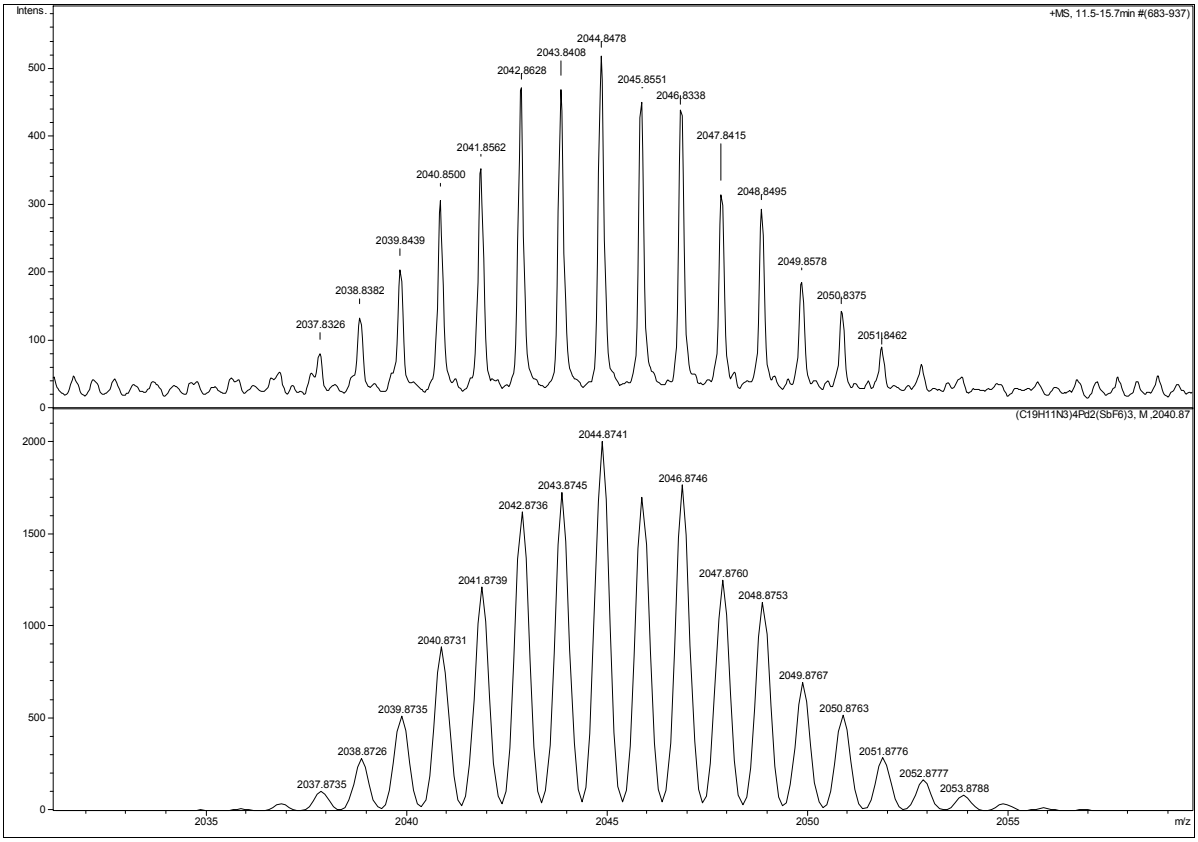

Figure S16: Experimental (top) and theoretical (bottom) isotope patterns for $[Pd_2(\mathbf{1})_4(SbF_6)_3]^+$.

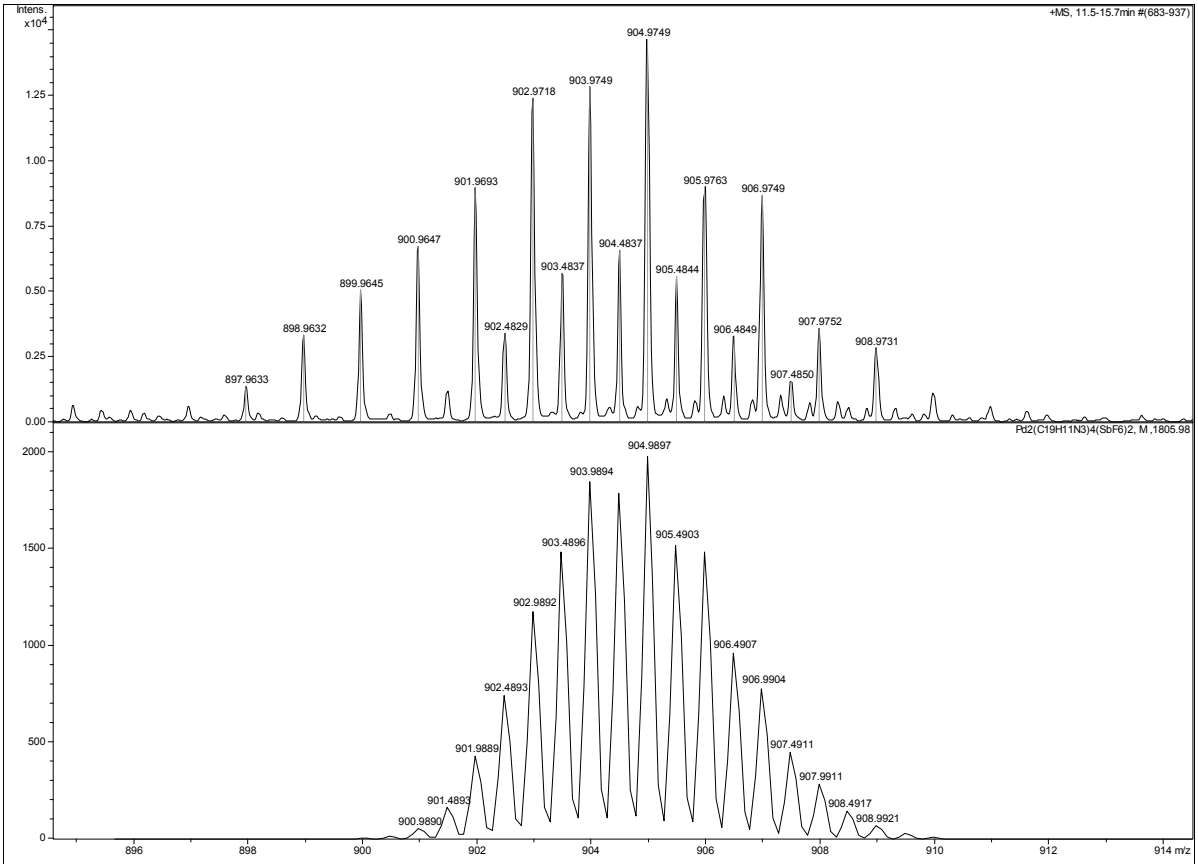

Figure S17: Experimental (top) and theoretical (bottom) isotope patterns for $[Pd_2(\mathbf{1})_4(SbF_6)_2]^{2+}$.

3.3 Mass Spectra of $[2\supset(\text{cisplatin})_2](BF_4)_4$

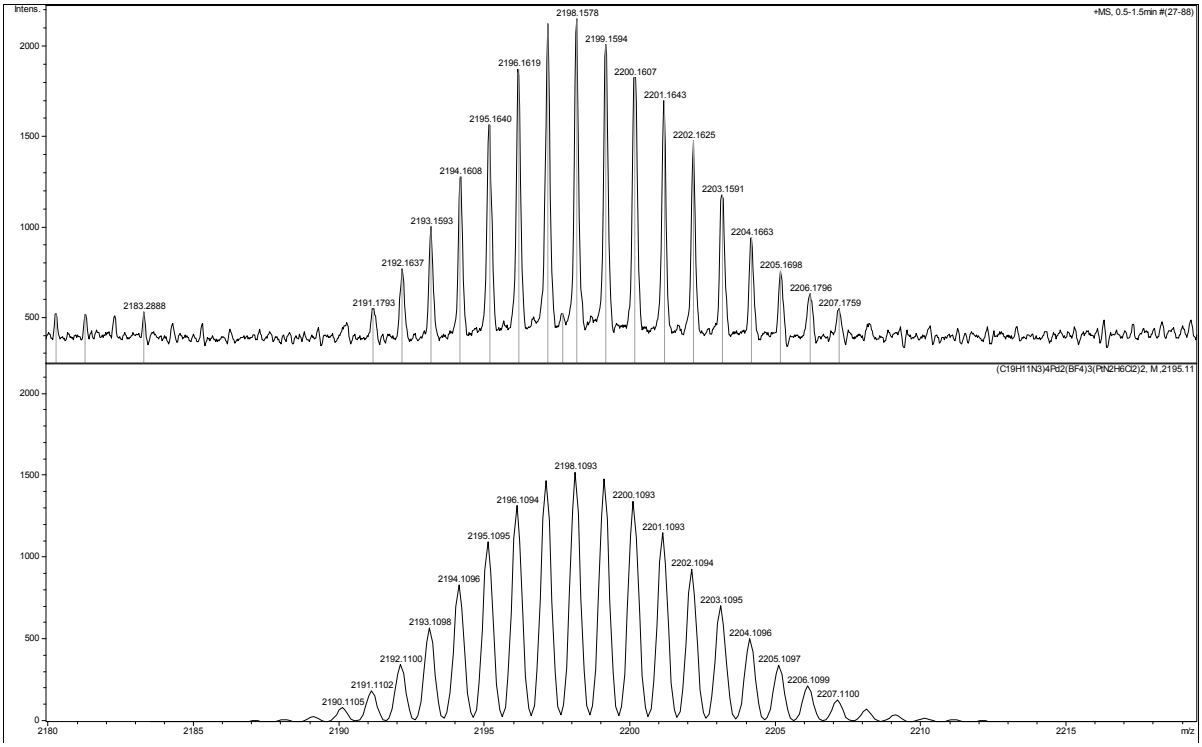

Figure S18: Experimental (top) and theoretical (bottom) isotope patterns for $\{\mathbf{2}(BF_4)_3\supset 2[Pt(NH_3)_2Cl_2]\}^+$.

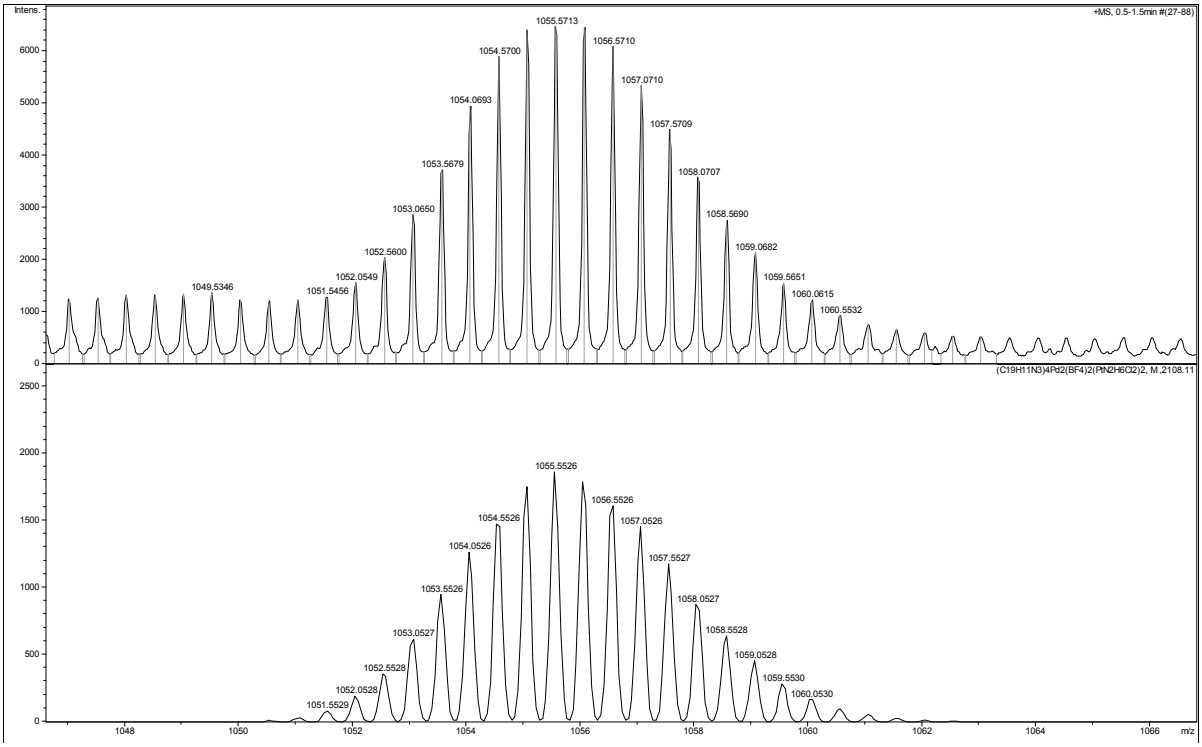

Figure S19: Experimental (top) and theoretical (bottom) isotope patterns for $\{\mathbf{2}(BF_4)_2\supset 2[Pt(NH_3)_2Cl_2]\}^{2+}$.

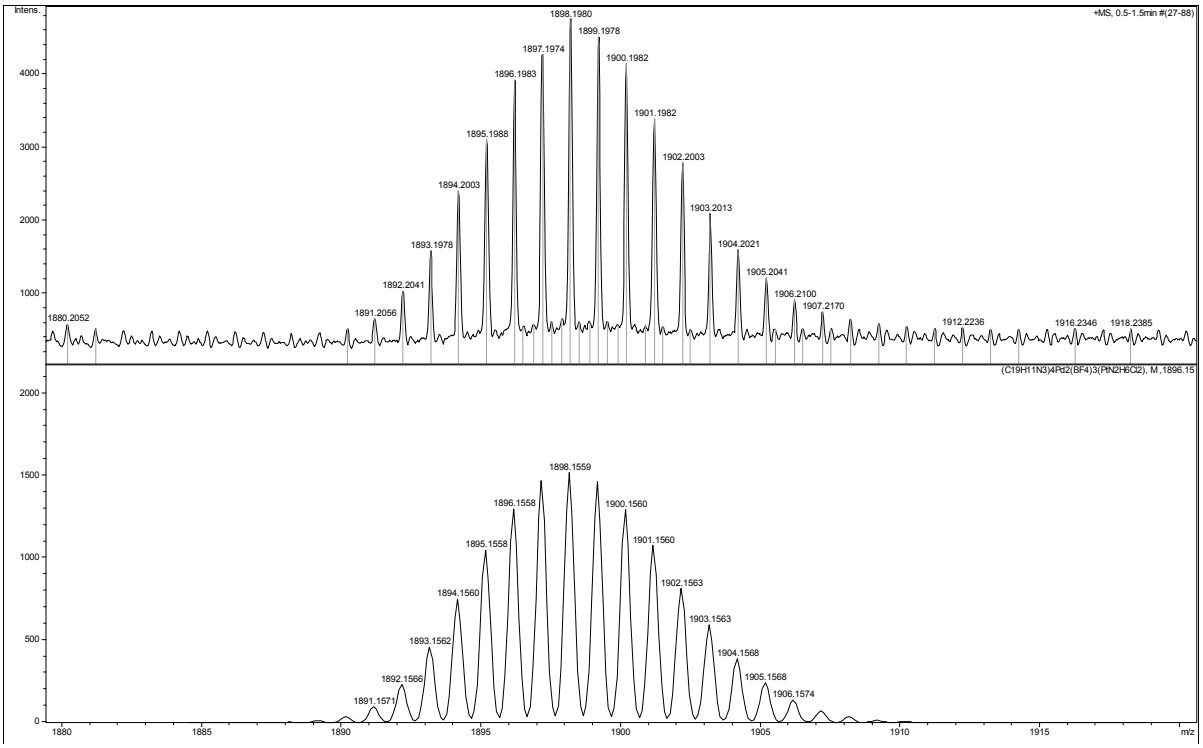

Figure S20: Experimental (top) and theoretical (bottom) isotope patterns for $\{\mathbf{2}(BF_4)_3 \supset [Pt(NH_3)_2Cl_2]\}^+$.

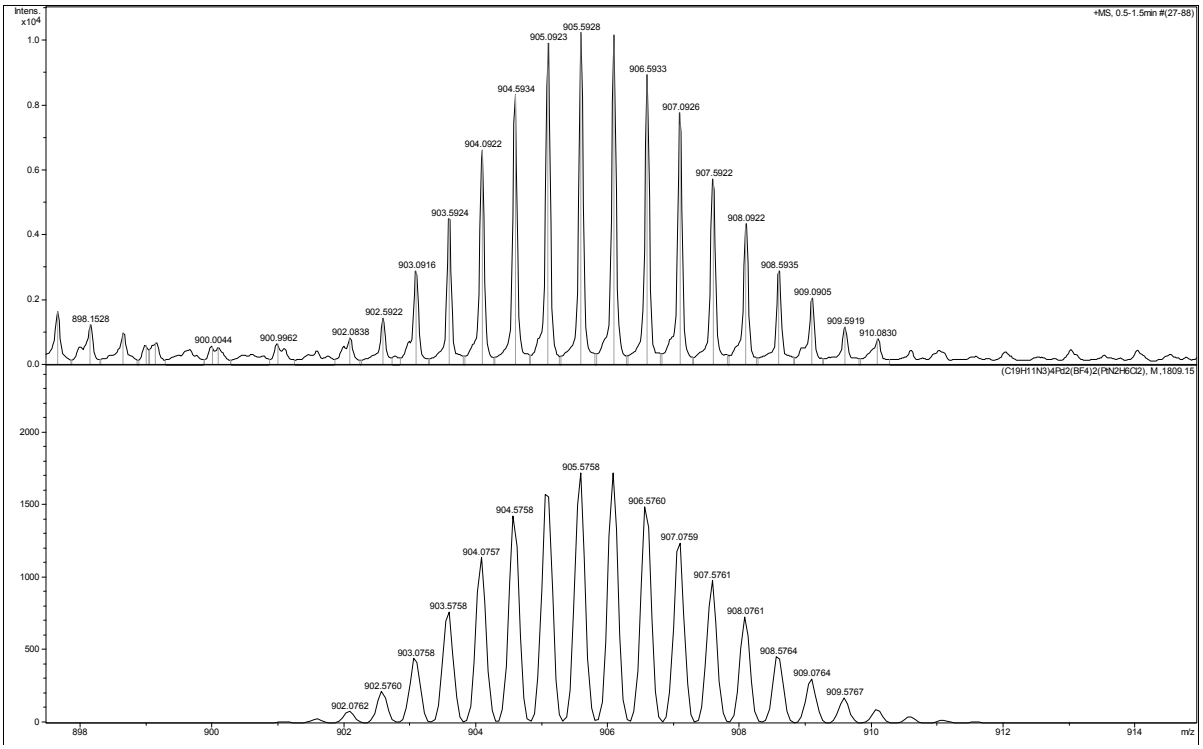

Figure S21: Experimental (top) and theoretical (bottom) isotope patterns for $\{\mathbf{2}(BF_4)_2 \supset [Pt(NH_3)_2Cl_2]\}^{2+}$.

3.4 Mass Spectra of $[Pd(DMAP)_4](BF_4)_2$

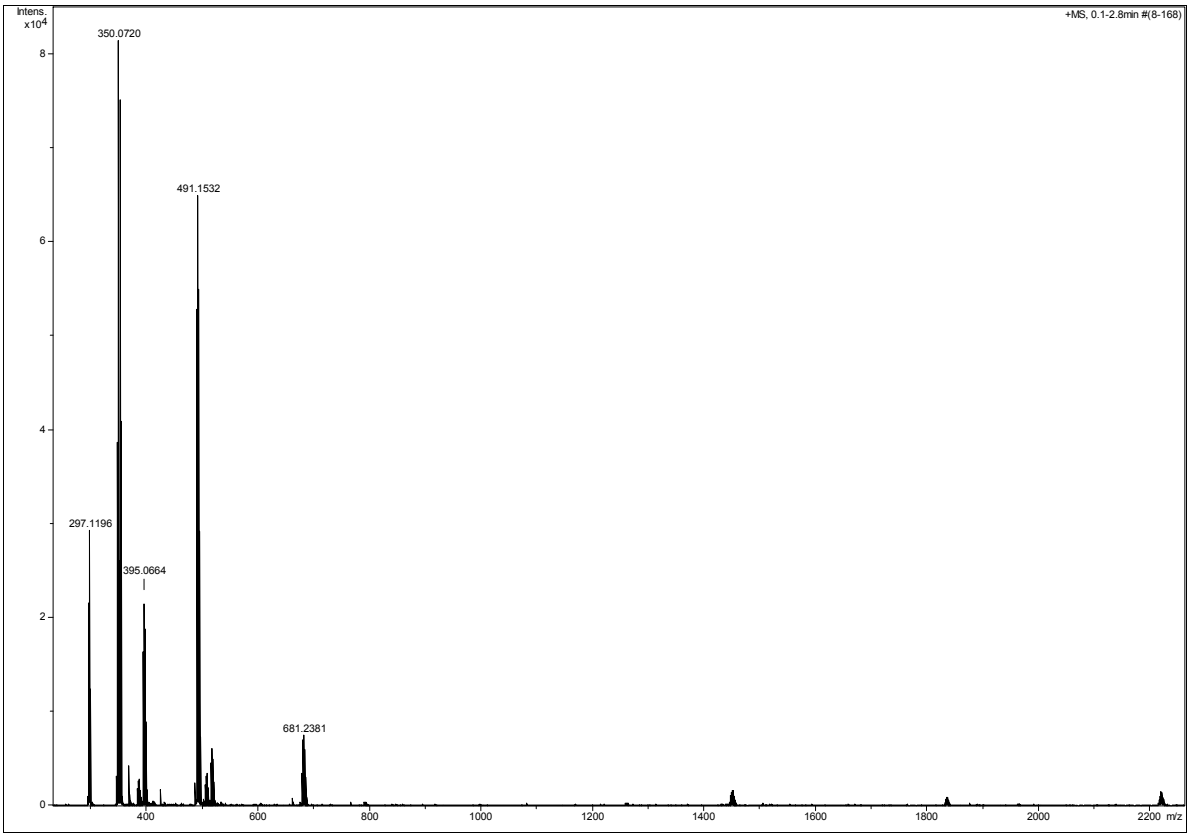

Figure S22: HR-ESI Mass Spectrum (+ve ion, MeCN) of $[Pd(DMAP)_4](BF_4)_2$. *m/z* = 681.2381 $[Pd(C_7H_{10}N_2)_4(BF_4)]^+$; 297.1205 $[Pd(C_7H_{10}N_2)_4]^{2+}$.

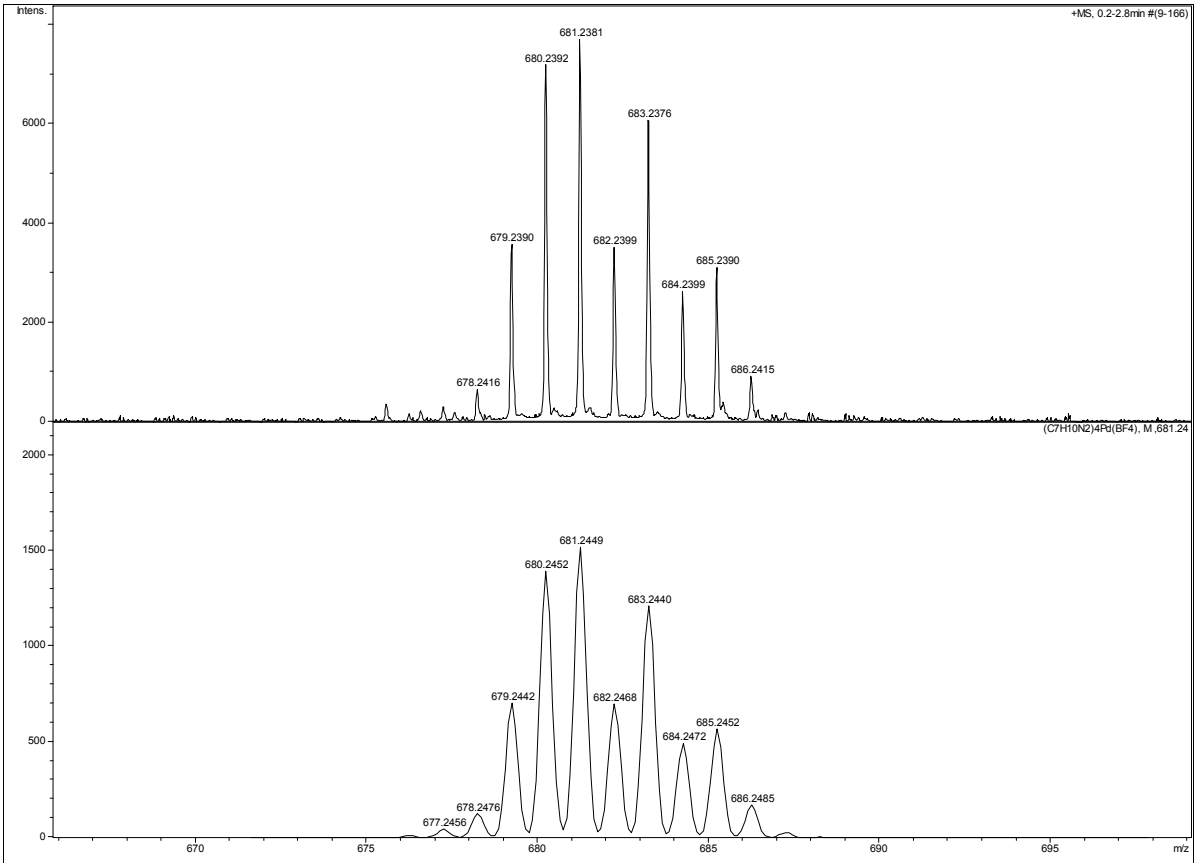

Figure S23: Experimental (top) and theoretical (bottom) isotope patterns for $[Pd(DMAP)_4](BF_4)^+$.

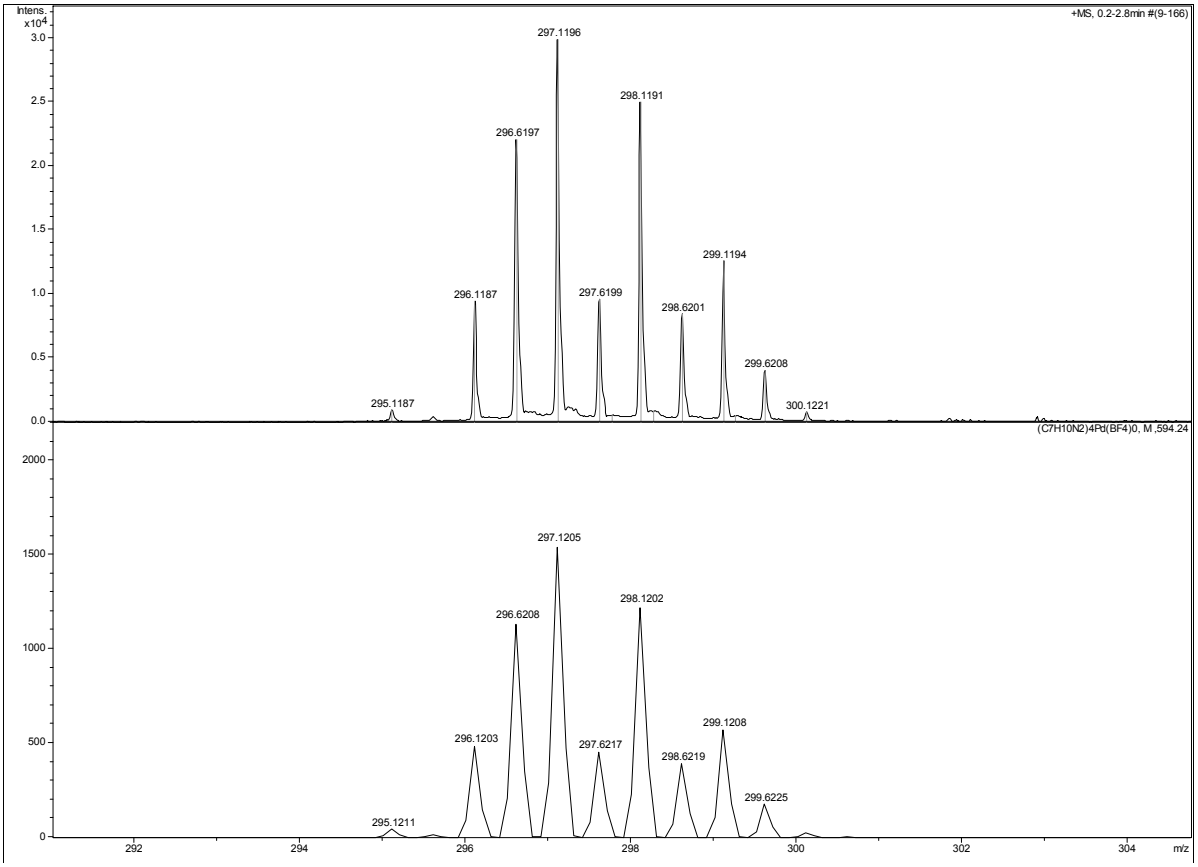

Figure S24: Experimental (top) and theoretical (bottom) isotope patterns for $[Pd(DMAP)_4]^{2+}$.

4 ^{1}H NMR Experiments

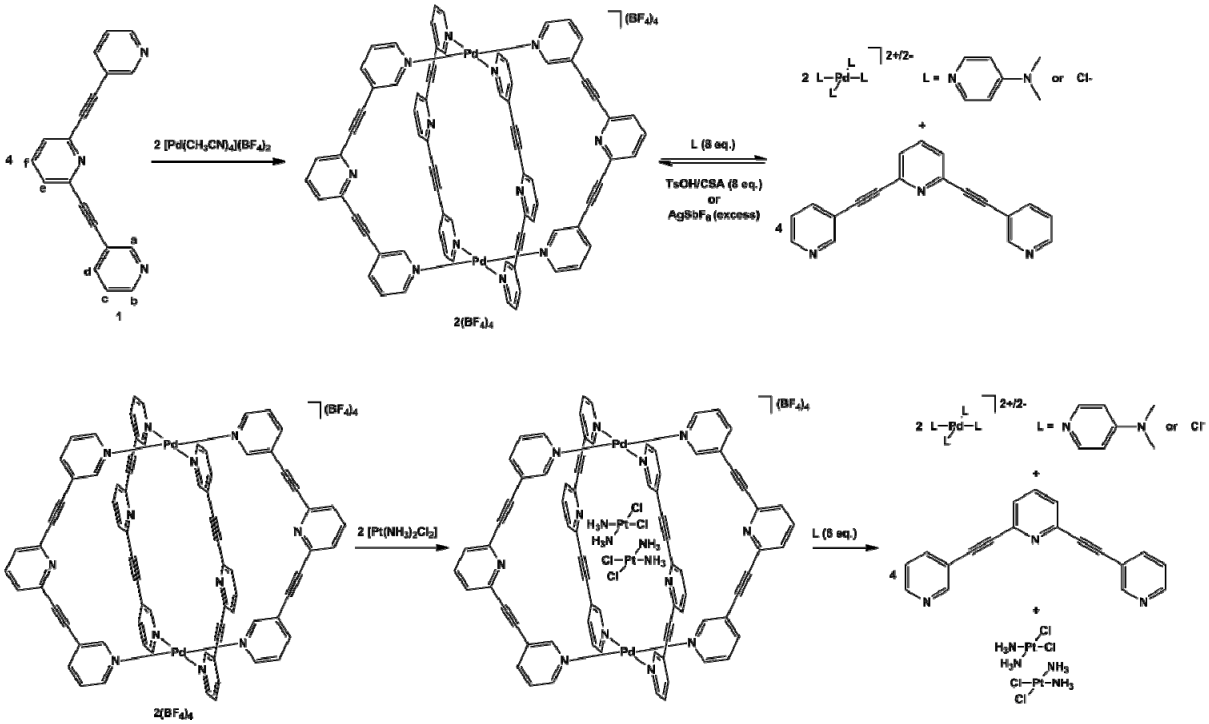

Figure S25: Reaction scheme for ^{1}H NMR disassembly/reassembly experiments.

4.1 $2(BF_4)_4$ + DMAP + Tosylic Acid (TsOH)

To a 17 mM solution of **2**$(BF_4)_4$ in d_6-DMSO (0.75 mL) was added DMAP (0.012 g, 0.1 mmol). After stirring for 5 minutes a ^{1}H NMR spectrum was obtained showing disassembly of the cage complex and formation of $[Pd(DMAP)_4](BF_4)_2$. The formation of $Pd(DMAP)_4$ and the presence of free ligand was confirmed by ESI-MS (Fig. S27). TsOH (0.017 g, 0.1 mmol) was added and the suspension gently heated until all solids were dissolved. A further ^{1}H NMR spectrum was obtained revealing protonation of DMAP and reassembly of **2**.

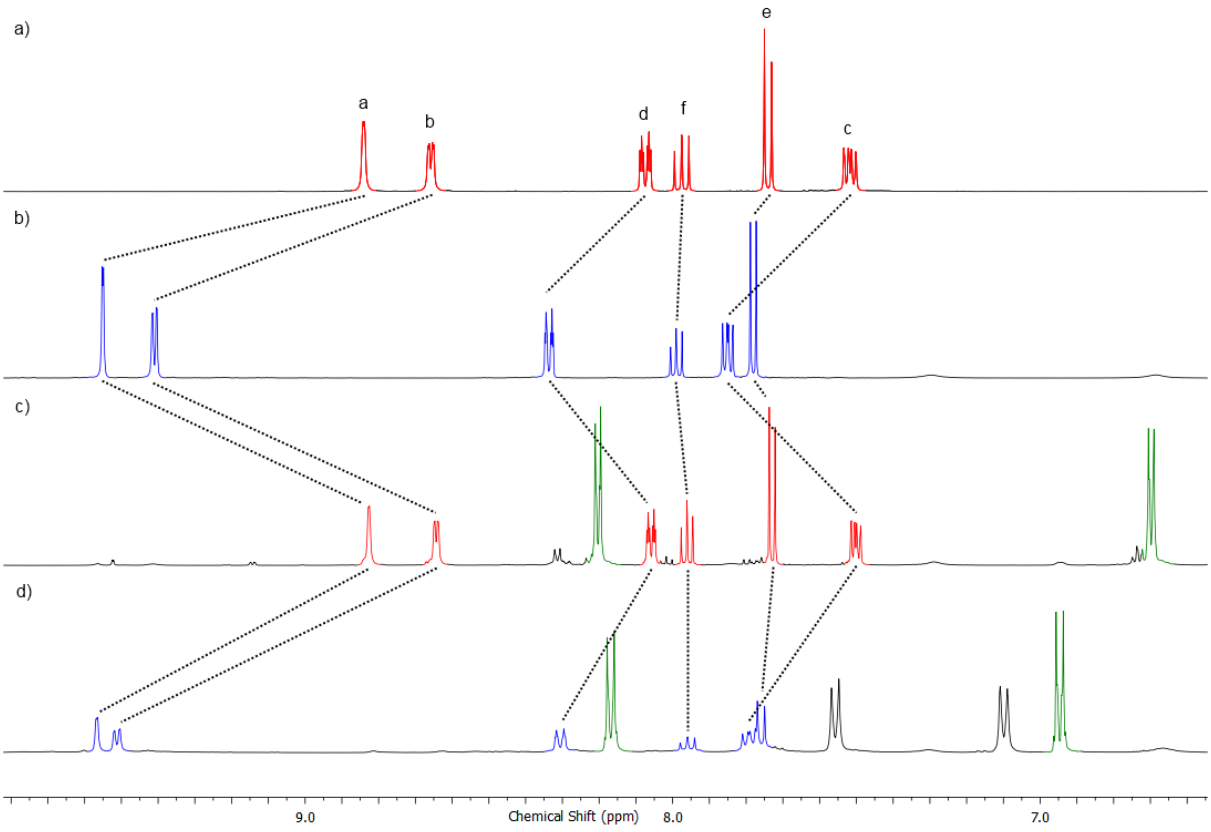

Figure S26: Stacked ^{1}H NMR (500 MHz, d_6-DMSO) spectra of a) **1**, b) **2**$(BF_4)_4$, c) **2**$(BF_4)_4$ plus DMAP (8 eq.), and d) **2**$(BF_4)_4$ plus DMAP plus TsOH (8 eq.). N.B. the signals for the reassembled cage differ slightly from the original due to interactions between the palladium cations and the sulfonate anions. This type of interaction has been studied and exploited extensively by Shionoya and co-workers.[1-3]

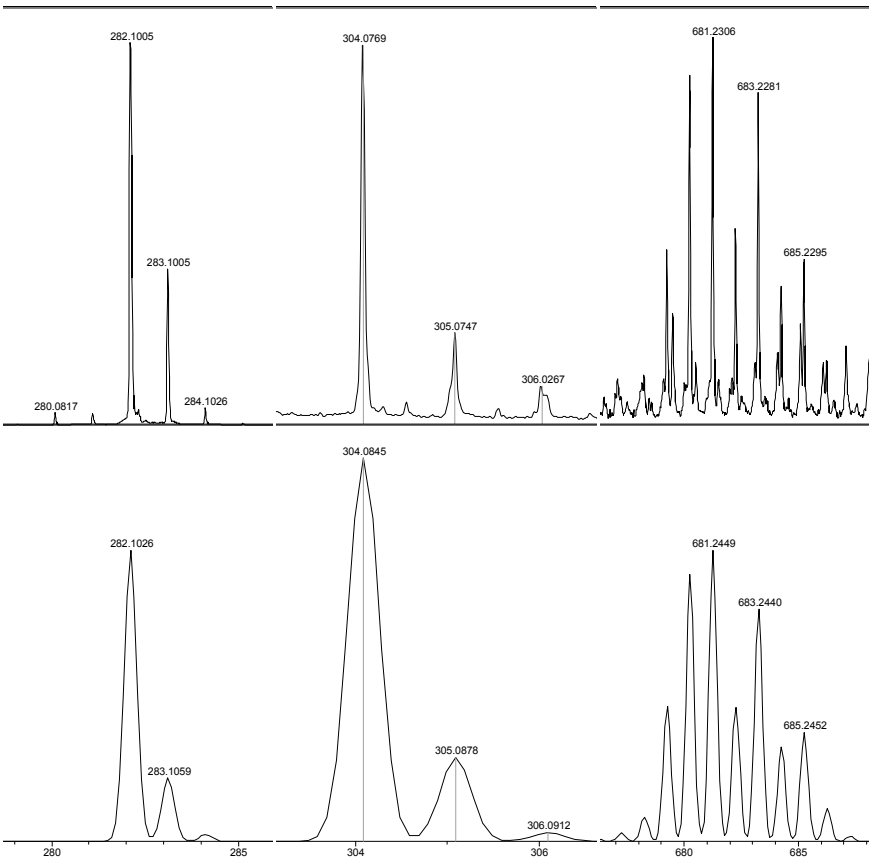

Figure S27: Experimental (top) and theoretical (bottom) isotope patterns for [**1**H]$^+$, [**1**Na]$^+$, and [Pd(DMAP)$_4$](BF$_4$)$^+$ (left to right respectively).

4.2 $2(BF_4)_4$ + DMAP + Camphor-10-sulfonic acid (CSA).

To a 4 mM solution of **2**$(BF_4)_4$ in CD_3CN (0.75 mL) was added DMAP (0.003 g, 0.02 mmol). After stirring for 5 minutes a ^{1}H NMR spectrum was obtained showing disassembly of the cage complex and formation of $[Pd(DMAP)_4](BF_4)_2$. CSA (0.006 g, 0.02 mmol) was added and the solution stirred for 5 minutes. A further ^{1}H NMR spectrum was obtained revealing protonation of DMAP. After 17 hours complete reassembly of **2** was observed.

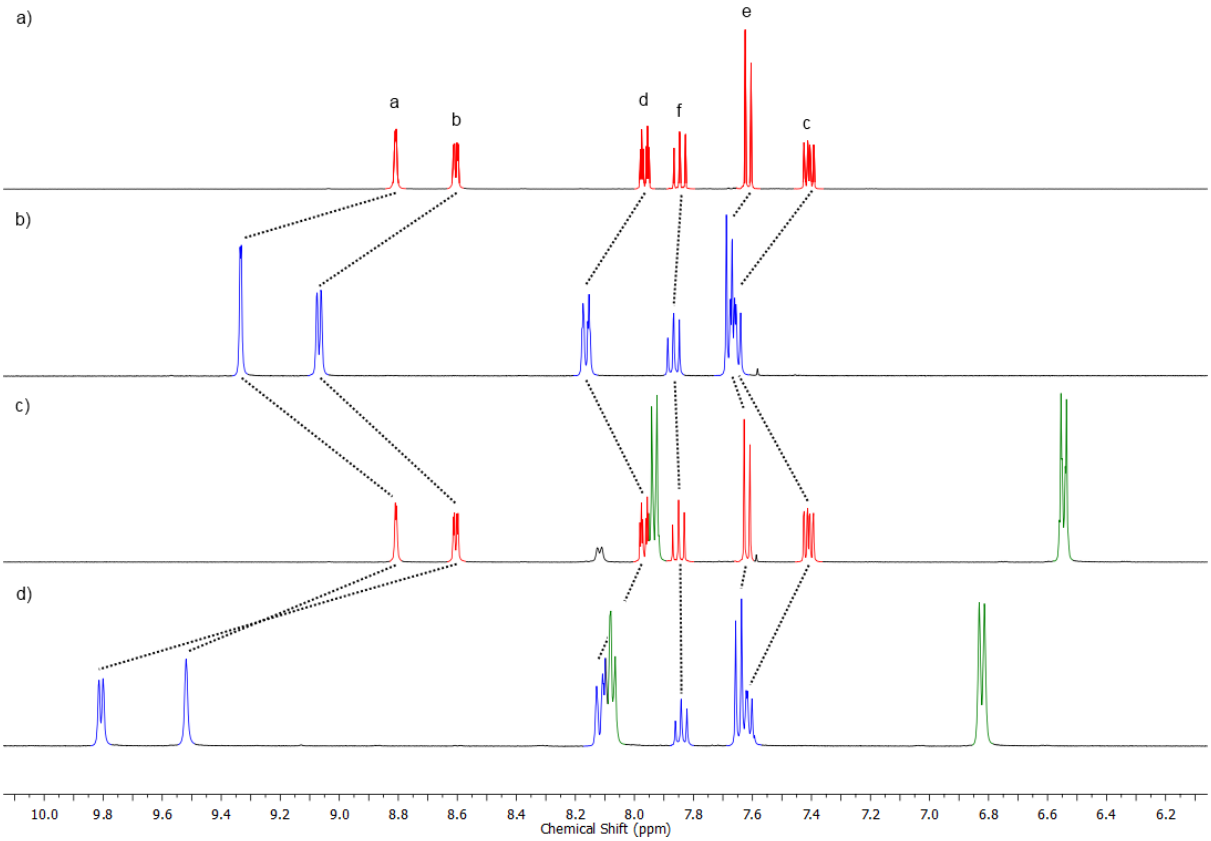

Figure S28: Stacked ^{1}H NMR (400 MHz, CD_3CN) spectra of a) **1**, b) **2**$(BF_4)_4$, c) **2**$(BF_4)_4$ plus DMAP (8 eq.), and d) **2**$(BF_4)_4$ plus DMAP plus CSA (8 eq.). N.B. the signals for the reassembled cage differ slightly from the original due to interactions between the palladium cations and the sulfonate anions. This type of interaction has been studied and exploited extensively by Shionoya and co-workers.[1-3]

4.3 $2(BF_4)_4$ + Bu_4NCl + $AgSbF_6$

To a 4 mM solution of **2**$(BF_4)_4$ in d_6-DMSO (0.75 mL) was added Bu_4NCl (0.007 g, 0.02 mmol). A precipitate was observed to form. A ^1H NMR spectrum was obtained showing disassembly of the cage complex. Upon addition of $AgSbF_6$ (0.008 g, 0.02 mmol) no change in the ^1H NMR spectrum was observed. Subsequent addition of further $AgSbF_6$ (0.020 g, 0.06 mmol) resulted in the reassembly of the cage complex.

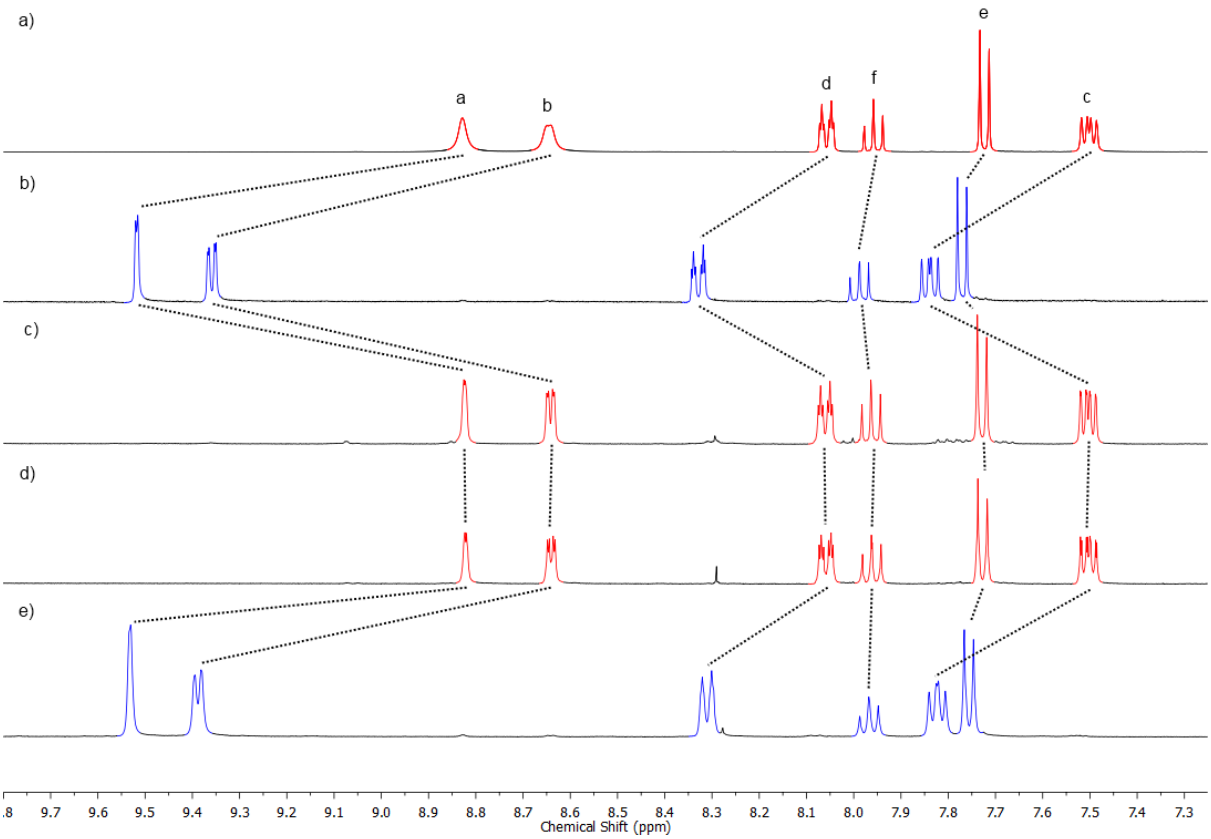

Figure S29: Stacked ^1H NMR spectra (400 MHz, d_6-DMSO) of a) **1**, b) **2**$(BF_4)_4$, c) plus Bu_4NCl (8 eq.), d) plus $AgSbF_6$ (8 eq.), and e) plus further $AgSbF_6$ (20 eq.).

4.4 $2(BF_4)_4$ + Cisplatin + Bu_4NCl

To a 4 mM solution of **2**$(BF_4)_4$ in CD_3CN (0.75 mL) was added cisplatin (0.002 g, 0.005 mmol) and the mixture sonicated for 10 minutes. A downfield shift and broadening of the H_a and H_b signals was observed in the ^1H NMR spectrum, indicative of encapsulation of cisplatin within **2**. Bu_4NCl (0.007 g, 0.02 mmol) was added to the reaction mixture. A precipitate was observed to form. A ^1H NMR spectrum was obtained showing disassembly of the host-guest complex.

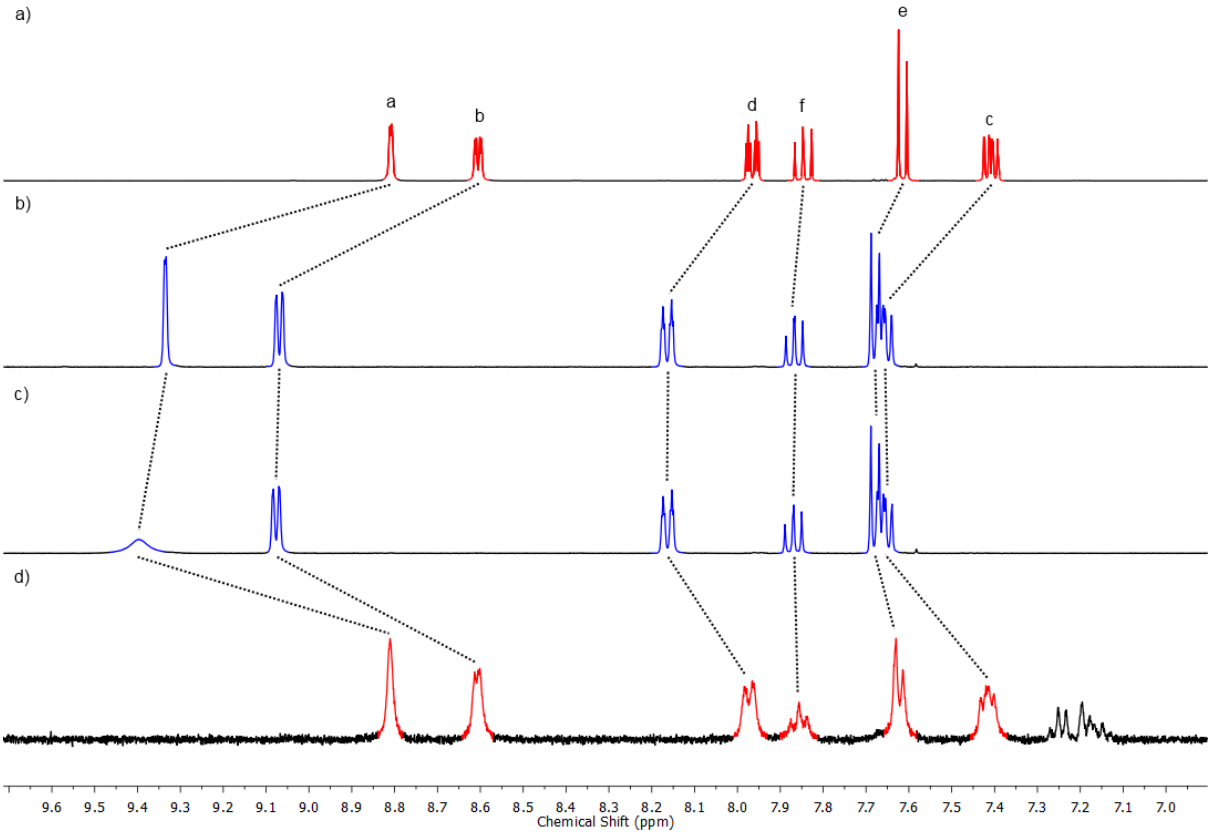

Figure S30: Stacked ^1H NMR spectra (400 MHz, CD_3CN) of a) **1**, b) **2**$(BF_4)_4$, c) host-guest adduct [**2**⊃$(cisplatin)_2$]$(BF_4)_4$, and d) plus Bu_4NCl (8 eq.).

5 Computer Modelling

5.1 SPARTAN Model of [2⊃(cisplatin)]

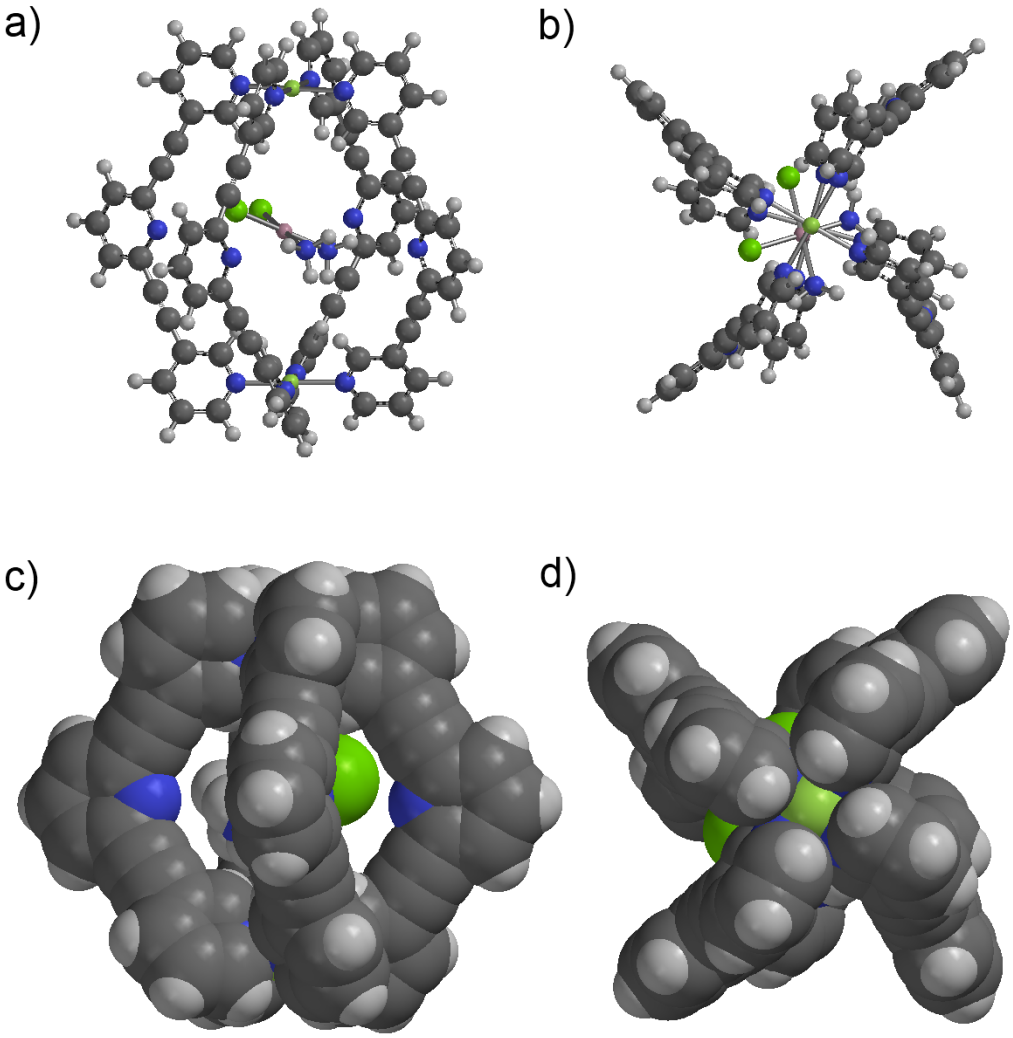

Figure S31: MMFF force field energy minimised SPARTAN model of [**2**⊃(cisplatin)]. Ball-and-stick representations viewed from a) the side, and b) the top; space-fill representations viewed from c) the side, and b) the top.

6 X-Ray Crystallographic Data

6.1 X-ray data collection and refinement for $2(SbF_6)_4$

X-ray data for **2**$(SbF_6)_4$ were collected at 89 K on a Bruker Kappa Apex II area detector diffractometer using monochromated Mo Kα radiation. The structure was solved by direct methods and refined against F^2 using anisotropic thermal displacement parameters for all non-hydrogen atoms (except where noted below) using APEX II software. Hydrogen atoms were placed in calculated positions and refined using a riding model.

The structure was solved in the primitive triclinic space group $P\bar{1}$ and refined to an R_1 value of 5.2%. Present in the asymmetric unit were two ligands bound orthogonally to a single Pd(II) atom, two hexafluoroantimonate counteranions (one of which is rotationally disordered), and multiple disordered solvent molecules (H_2O, acetone and MeOH).

The rotationally disordered hexafluoroantimonate counteranion was disordered over two sites with occupancies of 75% (F3 through F6) and 25% (F7 through F10). Sb1, F1 and F2 were all full occupancy. FLAT command was used to restrain F3 through F10 in the same plane. The quarter occupancy fluorine atoms did not behave well when refined anisotropically, thus were made isotropic.

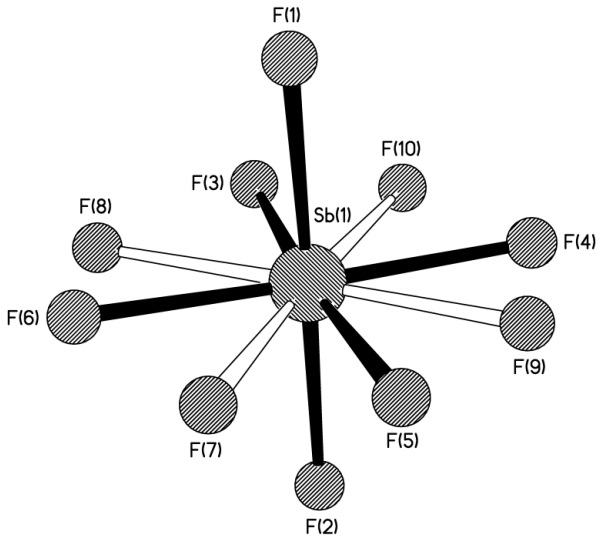

Figure S32: Ball-and-stick model of the rotationally disordered hexafluoroantimonate counteranion.

Inside the cage cavity were present four water and one methanol molecules. All were refined as full occupancy. Outside the cage were present three partial occupancy methanol molecules, a full occupancy methanol molecule disordered over three sites, and a full occupancy acetone molecule.

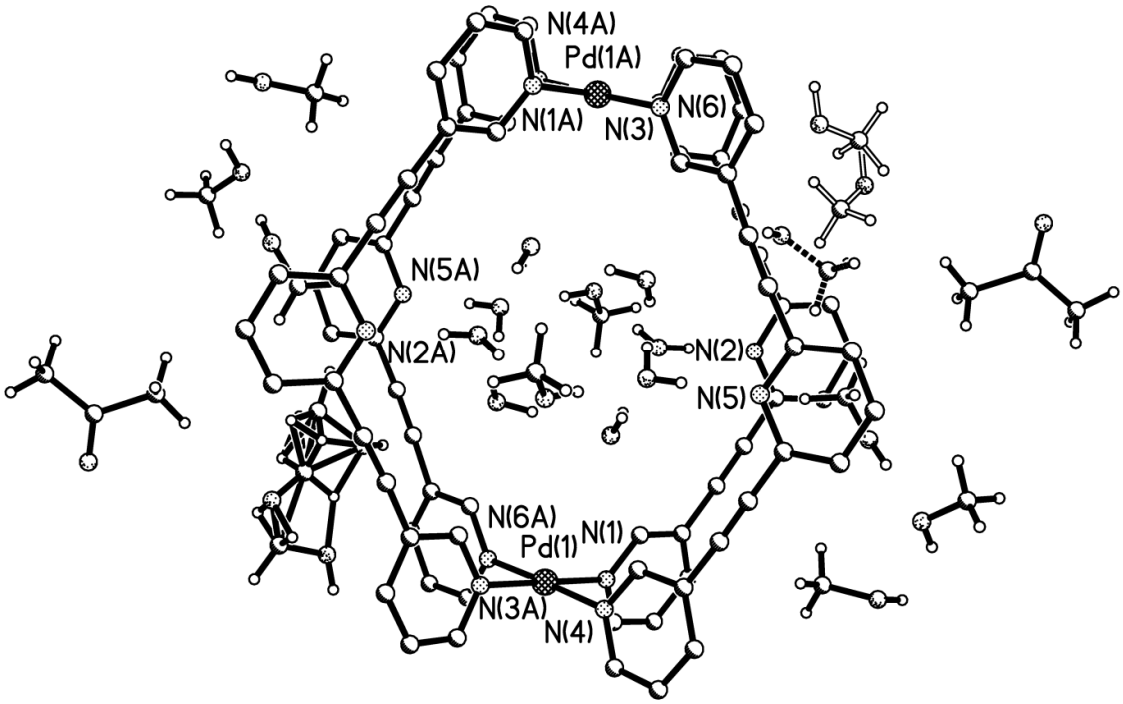

Figure S33: Ball-and-stick representation of the crystal structure of **2**$(SbF_6)_4$ showing disordered solvent molecules. SbF_6 counteranions and non-solvent hydrogen atoms have been removed for clarity.

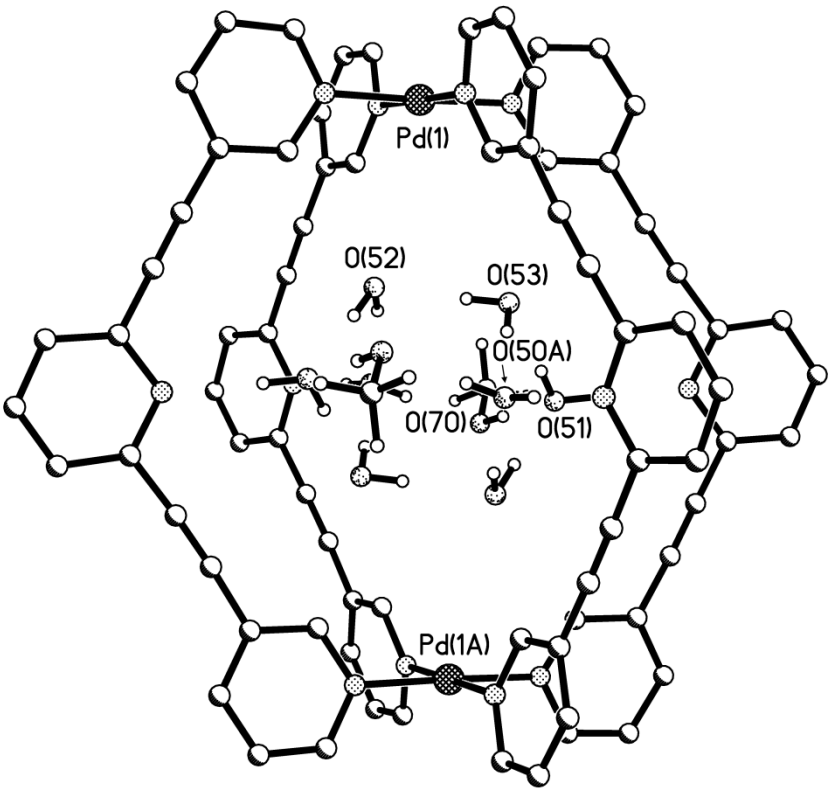

Figure S34: Ball-and-stick representation of the crystal structure of **2**$(SbF_6)_4$ showing disordered solvent molecules within the internal cavity of the cage complex. SbF_6 counteranions, external solvent molecules and non-solvent hydrogen atoms have been removed for clarity.

6.2 Table 1. Crystal data and structure refinement for $2(SbF_6)_4$.

Identification code	eg273	
Empirical formula	$C_{44.10}H_{48.40}F_{12}N_6O_{8.10}PdSb_2$	
Formula weight	1369.99	
Temperature	293(2) K	
Wavelength	0.71069 Å	
Crystal system	Triclinic	
Space group	$P\bar{1}$	
Unit cell dimensions	a = 12.850(5) Å	α= 66.868(5)°.
	b = 15.422(5) Å	β= 88.549(5)°.
	c = 16.768(5) Å	γ = 80.667(5)°.
Volume	3012.7(18) $Å^3$	
Z	2	
Density (calculated)	1.510 Mg/m^3	
Absorption coefficient	1.270 mm^{-1}	
F(000)	1352	
Crystal size	0.45 x 0.13 x 0.12 mm^3	
Theta range for data collection	1.46 to 20.68°.	
Index ranges	-12<=h<=12, -15<=k<=15, -16<=l<=16	
Reflections collected	55742	
Independent reflections	6112 [R(int) = 0.0854]	
Completeness to theta = 20.68°	98.6 %	
Absorption correction	Semi-empirical from equivalents	
Max. and min. transmission	0.7445 and 0.6373	
Refinement method	Full-matrix least-squares on F^2	
Data / restraints / parameters	6112 / 17 / 695	
Goodness-of-fit on F^2	1.096	
Final R indices [I>2sigma(I)]	R_1 = 0.0517, wR_2 = 0.1386	
R indices (all data)	R_1 = 0.0670, wR_2 = 0.1498	
Largest diff. peak and hole	1.145 and -0.684 e.$Å^{-3}$	

6.3 X-ray data collection and refinement for [**2**⊃(cisplatin)$_2$](BF$_4$)$_4$.

X-ray data for [**2**⊃(cisplatin)$_2$](BF$_4$)$_4$ were collected at 89 K on a Bruker Kappa Apex II area detector diffractometer using monochromated Mo Kα radiation. The structure was solved by direct methods and refined against F^2 using anisotropic thermal displacement parameters for all non-hydrogen atoms using APEX II software. Hydrogen atoms were placed in calculated positions and refined using a riding model.

The structure was solved in the primitive triclinic space group $P\bar{1}$ and refined to an R_1 value of 7.5%. One molecule of the host-guest adduct is present in the unit cell. ISOR command was used for atoms C1, C2 and C3. The tetrafluoroborate counteranions and solvent of crystallisation molecules were deemed too disordered to model. SQUEEZE was used to remove the aforementioned disorder, resulting in a void electron count of 374. With four tetrafluoroborate counteranions present totalling 168 electrons, the remaining 206 electrons can be accounted for by a variety of solvent molecule combinations from those solvents present, i.e. MeCN, DMF, Et_2O and H_2O (e.g. $(MeCN)_2(DMF)_3(Et_2O)$; $(MeCN)_8(H_2O)_3$).

In the asymmetric unit two ligands are bound orthogonally to a single Pd(II) atom and one cisplatin molecule is present. In the crystal lattice the molecules are arranged in an interlocking fashion with a centroid-centroid distance between the central pyridine moieties of 4.67 Å.

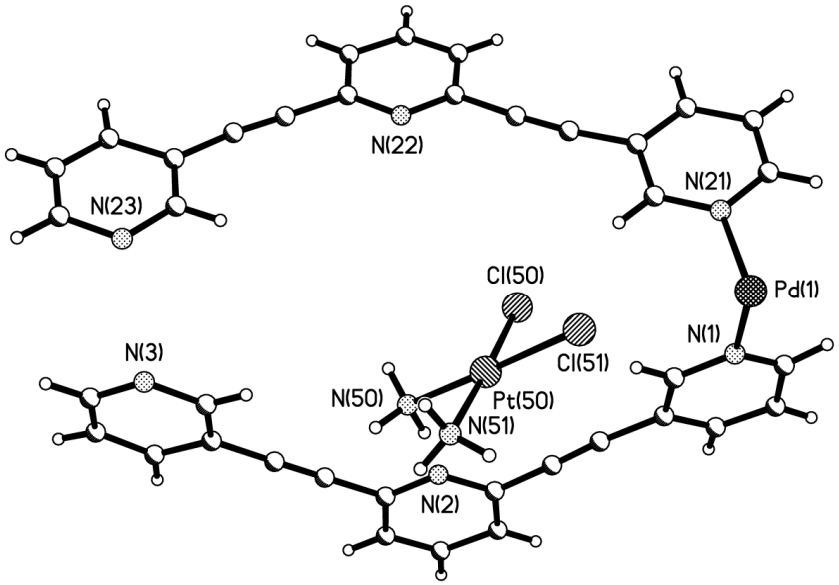

Figure S35: Ball-and-stick representation of the asymmetric unit cell of [**2**⊃(cisplatin)$_2$](BF$_4$).

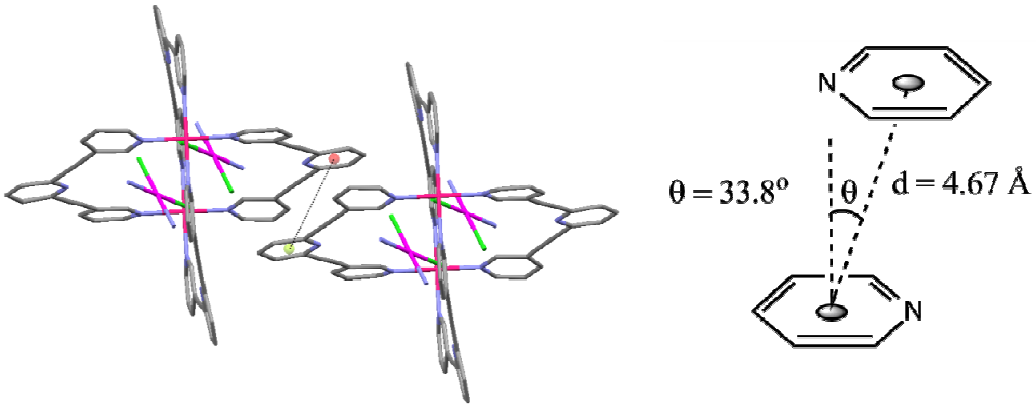

Figure S36: Capped-stick representation of interlocking between adjacent host-guest molecules in the crystal lattice of [**2**⊃(cisplatin)$_2$](BF$_4$)$_4$. Hydrogen atoms have been removed for clarity.

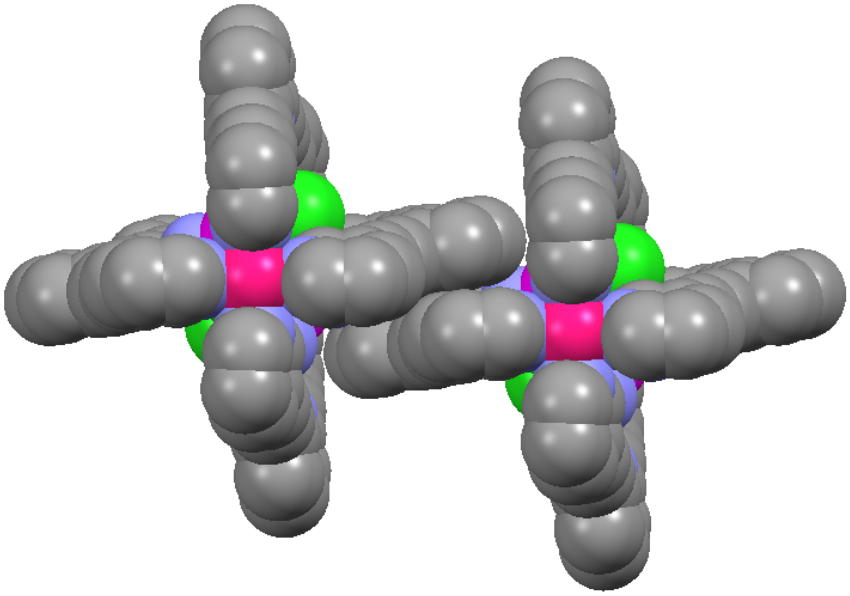

Figure S37: Space-fill representation of interlocking between adjacent host-guest molecules in the crystal lattice of [**2**⊃(cisplatin)$_2$](BF$_4$)$_4$. Hydrogen atoms have been removed for clarity.

6.4 Table 2. Crystal data and structure refinement for [2⊃(cisplatin)$_2$](BF$_4$)$_4$.

Identification code	jl_merged	
Empirical formula	C_{76} H_{56} C_{l4} N_{16} Pd_2 Pt_2	
Formula weight	1938.15	
Temperature	89(2) K	
Wavelength	0.71073 Å	
Crystal system	Triclinic	
Space group	$P\bar{1}$	
Unit cell dimensions	a = 11.9663(19) Å	α= 76.455(9)°.
	b = 12.3450(19) Å	β= 83.846(10)°.
	c = 17.495(3) Å	γ = 85.135(10)°.
Volume	2493.3(7) Å^3	
Z	1	
Density (calculated)	1.291 Mg/m^3	
Absorption coefficient	3.299 mm^{-1}	
F(000)	940	
Crystal size	0.32 x 0.32 x 0.31 mm^3	
Theta range for data collection	1.20 to 26.47°.	
Index ranges	-14<=h<=14, -15<=k<=15, -21<=l<=21	
Reflections collected	53506	
Independent reflections	10143 [R(int) = 0.0729]	
Completeness to theta = 26.47°	98.4 %	
Absorption correction	Semi-empirical from equivalents	
Max. and min. transmission	0.4278 and 0.4183	
Refinement method	Full-matrix least-squares on F^2	
Data / restraints / parameters	10143 / 18 / 454	
Goodness-of-fit on F^2	1.093	
Final R indices [I>2sigma(I)]	R_1 = 0.0748, wR_2 = 0.2226	
R indices (all data)	R_1 = 0.0965, wR_2 = 0.2379	
Largest diff. peak and hole	4.948 and -1.483 e.Å^{-3}	

6.5 Table 3. Squeeze results for [2⊃(cisplatin)$_2$](BF$_4$)$_4$.

Platon squeeze void nr	1
Platon squeeze void average x	0.500
Platon squeeze void average y	0.238
Platon squeeze void average z	0.923
Platon squeeze void volume	908
Platon squeeze void count electrons	374
Platon squeeze void content	Highly disordered BF_4 anions and solvent. The number of electrons is consistent with a number of combinations of solvent (H_2O, DMF, Et_2O and/or MeCN).

6.6 Space-filling representations of $2(SbF_6)_4$ and $[2\supset(cisplatin)_2](BF_4)_4$

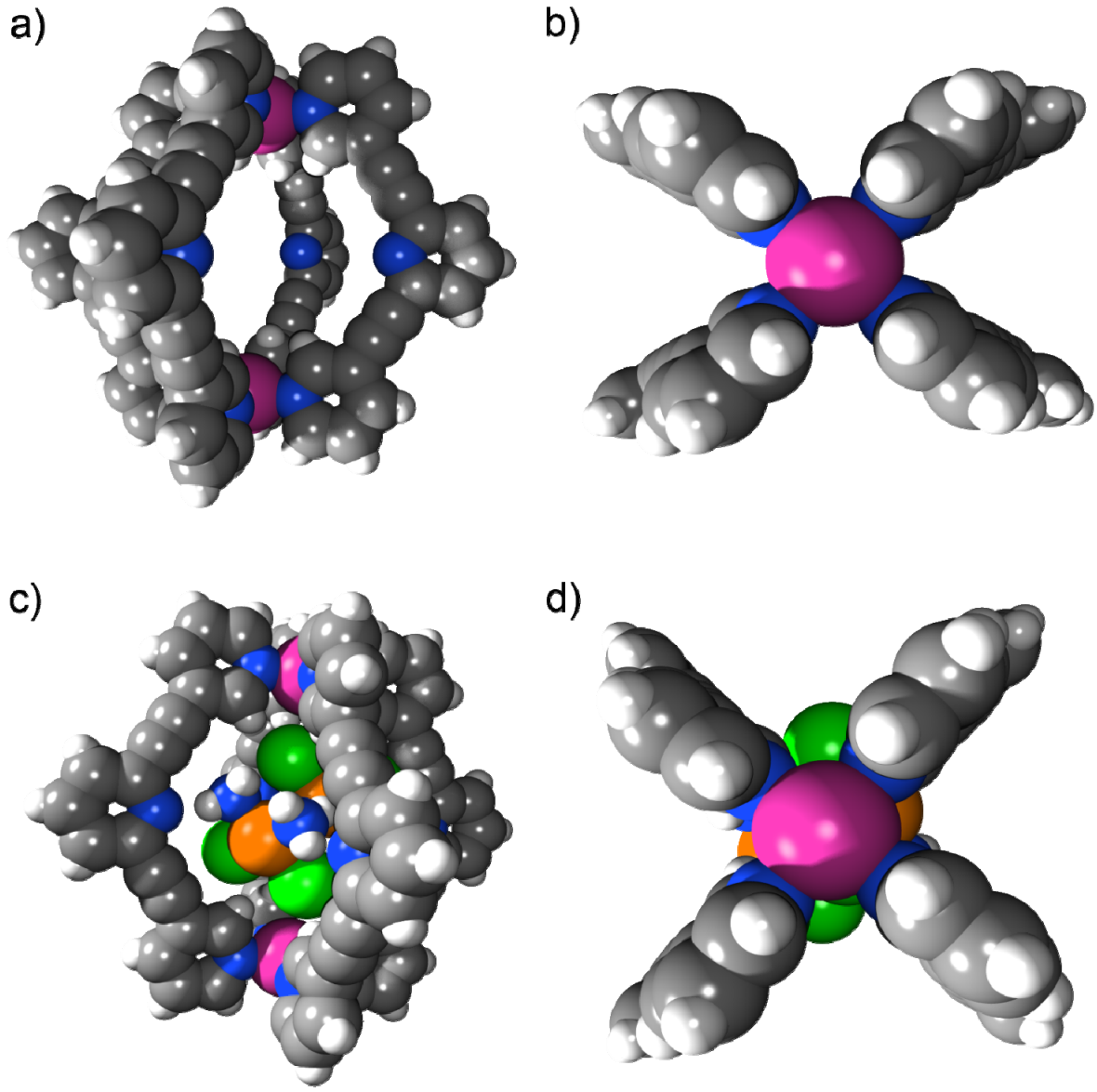

Figure S38: Space-filling representations of the crystal structures of **2**$(SbF_6)_4$ viewed from a) the side, and b) the top, and of [**2**$\supset$(cisplatin)$_2$]$(BF_4)_4$ viewed from c) the side, and d) the top. Counterions and solvent molecules had been removed for clarity.

---

7 References

(1) Clever, G. H.; Tashiro, S.; Shionoya, M. *Angew. Chem. Int. ed.* **2009**, *48*, 7010.
(2) Sakata, Y.; Hiraoka, S.; Shionoya, M. *Chem. Eur. J.* **2010**, *16*, 3318.
(3) Clever, G. H.; Tashiro, S.; Shionoya, M. *J. Am. Chem. Soc.* **2010**, *132*, 9973.